Published in final edited form as:

Curr Biol. 2020 February 03; 30(3): 465–479.e5. doi:10.1016/j.cub.2019.11.086.

A cycle of ubiquitination regulates adaptor function of the Nedd4-family ubiquitin ligase Rsp5

Chris MacDonald[1,2], **S. Brookhart Shields**[1,3], **Charlotte A. Williams**[1], **Stanley Winistorfer**[1], **Robert C. Piper**[1,*]

[1]Department of Molecular Physiology and Biophysics, University of Iowa, Iowa City, IA USA, 52242

[2]Current Address: Department of Biology, University of York, York, UK YO10 5DD

[3]Current Address: Gustavus Adolphus College, 800 West College Ave. Saint Peter, MN USA, 56082

SUMMARY

In yeast, the main ubiquitin ligase responsible for the sorting of proteins to the lysosomal vacuole is Rsp5, a member of the Nedd4 family of ligases whose distinguishing features are a catalytic HECT domain and 3 central WW domains that bind PY motifs in target proteins. Many substrates do not bind Rsp5 directly, and instead rely on PY-containing adaptor proteins that interact with Rsp5. Recent studies indicate that the activities of these adaptors are elevated when they undergo ubiquitination, yet the mechanism whereby ubiquitination activates the adaptors and how this process is regulated remain unclear. Here, we report on a mechanism that explains how ubiquitination stimulates adaptor function, and how this process can be regulated by the Rsp5-associated deubiquitinase, Ubp2. Our overexpression experiments revealed that several adaptors compete for Rsp5 *in vivo*. We found that the ability of the adaptors to compete effectively was enhanced by their ubiquitination and diminished by a block of their ubiquitination. Ubiquitination-dependent adaptor activation required a ubiquitin-binding surface within the Rsp5 catalytic HECT domain. Finally, like constitutively ubiquitinated adaptors, a Ubp2 deficiency increased both the adaptor activity and the ability to compete for Rsp5. Our data support a model whereby ubiquitinated Rsp5 adaptors are more active when “locked” onto Rsp5 via its N-lobe ubiquitin-binding surface, and are less active when they are “unlocked” by Ubp2-mediated deubiquitination.

eTOC Blurb

[*]Lead Contact: Robert-Piper@uiowa.edu.

AUTHOR CONTRIBUTIONS

CM, SBS, and RCP were responsible for the design and execution of experiments. CAW was responsible for executing the immunoprecipitation experiments. SW was responsible for constructing all plasmids. CM and RCP were primarily responsible for writing the manuscript and responding to reviewers’ comments.

DECLARATION OF INTERESTS

We declare no other conflicting interests

The HECT-type Ub ligase Rsp5 uses adaptor proteins to connect to substrates. MacDonald *et al.* show that adaptor ubiquitination strengthens association to Rsp5, focusing Rsp5 on cognate substrates while diverting it from non-cognate substrates. The deubiquitinating enzyme, Ubp2, may work to liberate Rsp5 to reprioritize adaptor associations.

Graphical Abstract

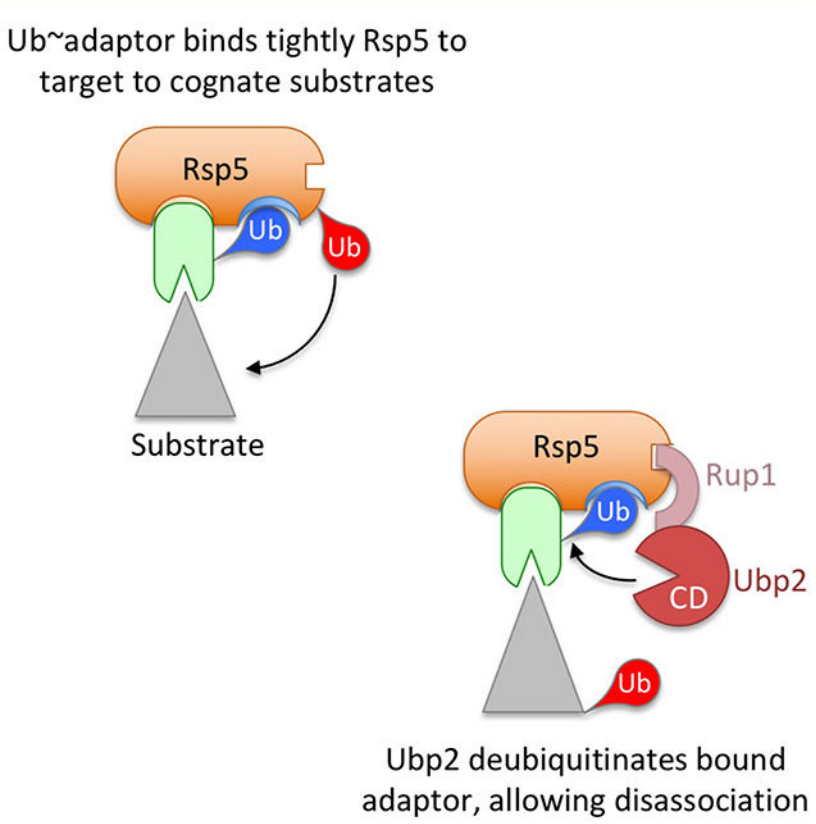

INTRODUCTION

Members of the Nedd4-related (neural precursor cell expressed, developmentally downregulated 4) ubiquitin (Ub) ligase family regulate a broad array of biological processes including the degradation of cell surface proteins by initiating their Ub-dependent sorting to the lumen of the endosome as well as trafficking to endosomes from the Golgi and plasma membrane [1, 2]. These ligases are characterized by an N-terminal lipid interacting C2 domain, between one and four protein-protein interaction WW domains, and a homologous to E6AP carboxyl terminus (HECT) catalytic domain, responsible for carrying a thiol-ester-linked Ub at its active site cysteine residue, which is ultimately transferred to substrates [3]. Whereas humans have nine Nedd4-family ligases, the yeast *Saccharomyces cerevisiae* has only one, Rsp5, which ubiquitinates a wide range of substrates [4, 5]. Although a variety of substrates can directly engage Nedd4-ligases by binding their WW domains using PY peptide (sequence [L/P]PxY) motifs, other substrates engage indirectly by binding adaptor proteins, which use their own PY motifs to bridge association with the ligase [5, 6]. Adaptor

proteins for Rsp5 include a diverse group of cytosolic proteins, many that share an arrestin-related motif, and also various membrane proteins such as Sna3 and Bsd2 that recruit Rsp5 to membrane proteins with which they associate [7–12].

How this complex system is regulated is not yet fully clear. First, many of the Rsp5-adaptor proteins become ubiquitinated themselves, as would be expected for proteins that directly associate with an active ligase [8, 13–15]. Yet, through an unknown mechanism, at least some of these adaptors require specific ubiquitination by Rsp5 to achieve their full activity [9, 16, 17]. Rsp5 also associates with the deubiquitinating enzyme Ubp2 using the bridging protein Rup1 [13, 18]. Whereas Rsp5 catalyzes formation of K_{63}-linked polyubiquitin chains, Ubp2 dismantles K_{63}-linked Ub-chains leading to the initial suggestion that Ubp2 simply antagonizes Rsp5 function. This is demonstrated in part by the hyperaccumulation of K63-polyubiquitin chains in *ubp2Δ* null mutants [18] and the ability of Ubp2 to diminish ubiquitination of Rsp5 substrates *in vitro* [13, 19]. However, loss of Ubp2 causes lysosomal trafficking defects for a wide range of membrane protein cargoes suggesting that Ubp2 somehow stimulates Rsp5 function [13, 20–22]. Finally, the HECT domain of Rsp5, as well as other Nedd4-family members, contains a site that mediates a non-covalent interactions with Ub and is required for full-activity of Rsp5 *in vivo* [23–26]. Here we propose a model that explains how these molecular features are coordinated to regulate Rsp5 activity, thereby distributing that activity appropriately to its many substrates and adaptors. Our data support a model whereby adaptors become ubiquitinated and bind tighter to Rsp5 via its WW motifs and Ub-binding surface. Tighter association with Rsp5 allows the adaptor to direct Rsp5 activity to only a subset of cognate targets, effectively depleting ubiquitination of non-cognate substrates. Ubp2 plays a contravening role to deubiquitinate adaptors, allowing them to disengage Rsp5 and thereby enable cycling of adaptors in response to distinct cellular requirements.

RESULTS

Hua1 is an Rsp5 adaptor that requires ubiquitination for full activity

Hua1 recruits Rsp5 to the ESCRT-0 complex (Vps27 and Hse1), which is part of the overall ESCRT apparatus required for sorting of ubiquitinated membrane proteins into the MVB pathway [21]. Association of Rsp5 with ESCRT-0 is required for the efficient MVB sorting of ubiquitinated cargo proteins such as Cps1. Hua1 helps recruit Rsp5 to ESCRT-0, by binding both Rsp5 and the SH3 domain Hse1. Rsp5 can also be recruited to ESCRT-0 via a direct interaction with the C-terminal PY motif of Hse1 (Figure 1A, S1A). Although loss of Hua1 alone has no discernable cargo sorting phenotype, loss of Hua1 does cause defects in MVB sorting in cells that express a mutant version of Hse1 that cannot directly bind Rsp5 [21]. Cps1 also relies on other mechanisms to engage Rsp5 for its efficient trafficking to the vacuole [27], consistent with the idea that Hua1 function is restricted to only a subset of cargoes engaging ESCRT-0 [21]. Thus, Hua1 serves as an adaptor for Rsp5, allowing Rsp5 activity to be localized near cargo undergoing MVB sorting. Mass spectrometry has previously shown Hua1 is ubiquitinated on the N-terminal residues K_3 and K_{18} [28, 29]. We confirmed that Hua1 was ubiquitinated, predominantly found as a monoubiquitinated species (Figure S1B, S1C). When expressed as an HA-epitope tagged protein (Figure 1B) or

a myc-epitope tagged protein (Figure 1C), a higher molecular weight species of Hua1 was readily isolated under denaturing conditions on Ni-NTA-linked sepharose using lysates from cells expressing 6xHis-tagged Ub. Similarly, the Rsp5 adaptors Rim8 and Ldb19 /Art1 could be observed in their ubiquitinated forms by this method, confirming previous studies showing these adaptors are ubiquitinated by Rsp5 to both regulate and in some cases, to induce degradation [9, 16, 30]. Previous experiments on other Rsp5 adaptors showed substitution of their ubiquitinated lysine with arginine diminished function [9, 16, 31]. This was also true for Hua1, which was revealed by comparing the function of wild-type Hua1 to a K_3R, $K_{18}R$ mutant lacking ubiquitinatable lysines ($Hua1^{K>R}$). Both versions of Hua1 were expressed under the native *HUA1* promoter, and both contained a modified myc epitope (myc*: EQRLISEEDL; which substituted the lysine in the original tag for arginine). The expression levels of both wild-type (WT) myc*-Hua1 and the myc*-$Hua1^{K>R}$ mutant were comparable by immunoblotting (Figure 1D, S1C), and overexposure of the blot allowed detection of a slower migrating band corresponding to the ubiquitinated form for WT myc*-Hua1, which was not observed for myc*-$Hua1^{K>R}$. In cells lacking Hua1 and also carrying an Hse1 mutant lacking is PY Rsp5-binding motif (*hse1*$^{\Delta rsp5}$), expression of myc*-Hua1 restored MVB sorting of GFP-Cps1 but expressing the myc*-$Hua1^{K>R}$ mutant did not (Figure 1E). Together, these results suggest that like other Rsp5 adaptors [9, 16, 17], Hua1 requires ubiquitination to become fully active.

Adaptor protein over-expression interferes with non-cognate Rsp5-dependent processes

Preliminary experiments indicated that overexpression of Hua1 caused dominant negative effects on other Rsp5-dependent processes. These data implied that overexpression of Hua1 competes and displaces other adaptors from Rsp5, with a concomitant decrease in ubiquitination of their respective substrates. Such observations are consistent with the previous observations showing overexpression of Rsp5 adaptors inhibits MVB sorting of their non-cognate cargoes [8, 32–34]. We exploited this observation to further investigate the effect of ubiquitination of Hua1. We compared the effects of overexpressing Hua1 with a Ub-Hua1 fusion, in which Ub (aa 1–75) was fused to the N-terminus of Hua1 to mimic a constitutively ubiquitinated form of Hua1 (Figure 2A). As a control, we included a truncation mutant of Hua1 ($Hua1^{\Delta N}$) in which the N-terminal region containing the K_3 and K_{18} ubiquitination sites, as well as an Rsp5-binding PY motif were removed. The levels of each of these constructs from a low copy plasmid were assessed following induced expression from the *CUP1* promoter (Figure 2B, S2D). The level of WT myc-Hua1 was comparable to that of the myc-tagged $Hua1^{\Delta N}$, whereas the levels of the myc-tagged Ub-Hua1 fusion were distinctly lower. Increased exposure showed that myc-Hua1 had additional ubiquitinated species, including a band that co-migrated with Ub-Hua1 and a higher band consistent with di-ubiquitinated Hua1 in each lane, indicating that a portion of myc-Hua1 was ubiquitinated. $Hua1^{\Delta N}$ showed no evidence of ubiquitination (Figure 2B). Overexpressing Hua1 inhibited growth at 37°C and growth inhibition was even more profound upon overexpressing Ub-Hua1 (Figure 2C). Although this difference was observed at different levels of copper induction, we presume inhibition of Ub-Hua1 is near maximal, because very high copper levels copper levels were required for Hua1 to cause defects as severe as Ub-Hua1 (Figure S1E). In contrast, overexpressing $Hua1^{\Delta N}$ or $Hua1^{K>R}$ mutants that do not get ubiquitinated had no effect (Figure 2D). Hua1 overexpression caused defects

in the Rsp5-dependent sorting of GFP-tagged membrane proteins along the MVB pathway into the vacuolar lumen. In general, these defects were more pronounced upon expression of the 'constitutively ubiquitinated' Ub-Hua1 fusion protein and were absent upon expression of the Hua1$^{\Delta N}$ mutant. We found that overexpressing Hua1 and Ub-Hua1 had profound defects in sorting Sna3-GFP to the vacuole (Figure 2E). We and others have previously shown that Rsp5-dependent mono-and di-ubiquitinated species of Sna3 are detectable by immunoblot [35, 36]. We took advantage of this to show that the levels of Sna3-HA are stabilized in Hua1-overexpressing cells, whilst the relative proportion of ubiquitinated Sna3-HA was reduced (Figure 2F, S2A–C). Overexpressing Ub-Hua1 diminished the proportion of ubiquitinated Sna3 to the same extent as Hua1 overexpression despite its dramatically reduced levels, suggesting the inhibitory effects of Ub-Hua1 were more potent. Similarly, overexpressing Hua1 caused mis-sorting of GFP-Cps1 and Gap1-GFP, yet had little effect on Ste3-GFP or Mup1-GFP in the presence of methionine. In contrast, expressing Ub-Hua1 caused mis-sorting of all of these cargoes and caused a more severe phenotype for Gap1-GFP (Figure 2G). We further note that expression of Ub-Hua1 appears to elevate levels of surface cargoes (Ste3, Gap1, Mup1) at the plasma membrane when compared with Hua1 overexpression, suggesting the more efficient ubiquitinated competitor interfere with Ub-dependent membrane trafficking steps that ultimately lead proteins into the vacuole [2]. These effects can collectively be explained by Hua1 titrating available Rsp5, competing away adaptors, such as Bul1/2 or Art1 that mediate Rsp5-dependent ubiquitination of Gap1 and Mup1, respectively, or the ability of Rsp5 to engage Sna3 and Cps1 directly through their Rsp5 binding motifs [27, 35]. Moreover, Ub-Hua1 was more potent in causing these effects, highlighting the importance of ubiquitination in the ability of Hua1 to affect Rsp5 function. We also examined the effects of Hua1 overexpression on another Rsp5-dependent process, the proteolytic processing of Rim101 into an active transcription factor in response to alkaline stress, which requires the arrestin-related Rsp5 adaptor Rim8 [17, 32]. In cells shifted from pH 3.5 to pH 8.0 for 25 minutes, Rim101-HA was processed to a lower molecular weight form as predicted. Yet, overexpression of Hua1 and Ub-Hua1 blocked alkaline-induced processing of Rim101-HA (Figure 2H). We note that the extent of Rim101 processing varies among different parental strains (Figure S3A), yet the ability of Hua1 overexpression to inhibit Rim101 processing was observed for both strains tested.

Cognate activities of adaptors proteins are stimulated by ubiquitination

We next determined how these observations could be extended to explain the function of other Rsp5 adaptors. Art1 is an Rsp5 adaptor that promotes ubiquitination and sorting of Mup1 and Can1 into the vacuole lumen, a process that is induced by their respective substrates methionine and arginine (Figure 3A). Art1 undergoes ubiquitination on K_{486} and a $K_{486}R$ mutant has a diminished ability to mediate Rsp5-dependent sorting of Can1 to the vacuole [9]. Consistent with these studies, we found that a portion of overexpressed HA-epitope-tagged Art1 was ubiquitinated, whereas no ubiquitinated species was observed for the overexpressed $K_{486}R$ mutant (Art1-HA$^{K>R}$) construct (Figure 3C). Overexpression of Art1-HA caused Mup1 to traffic to endosomes in media lacking exogenous methionine, showing that Art1 overexpression partially bypassed the requirement of substrate induced Mup1 downregulation (Figure 3B). This effect was far more dramatic upon overexpression of Art1-HA-Ub fusion protein, where Ub ($G_{76}S$) was fused onto the C-terminus. Here,

Mup1-GFP sorted more efficiently through the MVB pathway to accumulate within the vacuole. This enhanced activity of Art1-Ub towards its cognate cargo Mup1 was not due to a level of expression that was higher than Art1-HA alone (Figure S2D). In contrast, overexpressing Art1-HA^{K486R} to levels comparable to WT Art1-HA had no effect on Mup1-GFP sorting (Figure 3B, 3C). To verify the role of Rsp5 in vacuolar sorting of Mup1-GFP, we found antagonizing Rsp5 activity with fusion of a deubiquitinating enzyme [35], even in the presence of methionine, completely blocked Mup1-GFP sorting. A similar pattern was found in the ability of Art1 to inhibit non-cognate processes when overexpressed (Figure 3D). Expressing myc-Art1 from the copper inducible *CUP1* promoter inhibited growth at 37°C mirroring the in hibitory effects on growth resulting from overexpressing Hua1. Although expressed to similar levels, the myc-epitope-tagged Art1^{K486R} did not cause a growth defect at elevated temperature. Similarly, overexpressing Art1-HA had a slight yet discernable defect in MVB sorting of GFP-Cps1, which uses an Art1-independent means of recruitment to Rsp5 [21, 27]. This dominant-negative sorting defect was very dramatic upon expressing an Art1-HA-Ub fusion protein, whereas no defect was observed upon overexpressing Art1-HA^{K486R}, again underscoring the role ubiquitination plays on the ability of Art1 to co-opt Rsp5 (Figure 3G). We also examined Rim8, an Rsp5 adaptor that conveys signals from a plasma membrane protein complex containing Rim21 to the proteolytic processing of the Rim101 transcription factor [37], a pathway that is normally triggered when cells are shifted from acidic to alkaline growth conditions (Figure 3E). We found that overexpressing V5-epitope-tagged Rim8 was sufficient to cause Rim101 processing in cells maintained in acidic growth conditions, showing that an excess of Rim8 allowed it to bypass the normal trigger of alkaline shift (Figure 3F, S3B). Rim8 is known to be ubiquitinated at K_{521}, and overexpressing a Rim8 $K_{521}R$ mutant (Rim8$^{K>R}$) had no effect on promoting promiscuous Rim101 processing in acidic conditions. The effect of overexpressing Rim8 on its non-cognate substrate GFP-Cps1 mirrored the effects observed for Art1. Rim8-V5 expression caused minor defects in sorting of GFP-Cps1, yet overexpression of Rim8-V5-Ub, a ‘constitutively ubiquitinated’ version of Rim8 in which Ub($G_{76}S$) was fused to the C-terminus, caused a profound defect in GFP-Cps1 sorting (Figure 3G) despite the fact that the overall levels of Rim8-V5-Ub were demonstrably lower that the WT Rim8-V5 protein (Figure 3F).

Ubiquitinated adaptors regulate Rsp5 activity via direct binding

Consistent with previous observations [10, 11, 33, 38, 39], the above data indicate that Rsp5 is limiting and that adaptors compete for occupancy on Rsp5 to effectively direct activity to their substrates. Consequently, this would diminish the ability of Rsp5 to work with other adaptors that target non-cognate substrates and processes. To explain these effects we considered a model in which ubiquitination of Rsp5 adaptors allows them to lock onto Rsp5, with enhanced engagement through the WW domains of Rsp5 in combination with the non-covalent Ub-binding surface (UBS) within the N-lobe of the HECT catalytic domain, which has been described for a number of HECT domains including that of Rsp5 [24–26, 40]. This can explain how Rsp5 adaptors appear more functionally active towards their cognate substrates and how they can better compete against other Rsp5 adaptors when they are ubiquitinated (Figure 4). As confirmation that the dominant-negative effects of Hua1 overexpression are mediated through its ability to work as a competitive Rsp5 inhibitor, we

found that the inhibitory effects of myc-Hua1 overexpression on growth at 37°C were suppressed by overexpression of Rsp5 (Figure 5A). In addition, overexpressing Rsp5 suppressed the defect in downregulation of Ste3-GFP caused by overexpressing myc-Ub-Hua1, diminishing the plasma membrane localization of Ste3 (Figure 5B). This was also observed using an assay that couples mating efficiency to the turnover of cell surface Ste3 (Figure 5C, 5D, S3E). Here, production of Ste3 is under control of the *GAL1* promoter, which allows the synthesis of new Ste3 to be blocked when cells are shifted from galactose to dextrose, and the ability to mate at increasing times after the shift is proportional to the level of pre-existing Ste3 that resists downregulation and remains at the cell surface [41]. In cells carrying vector or Hua1$^{\Delta N}$, mating was virtually abolished after 20 min of growth in dextrose. However, cells overexpressing myc-Ub-Hua1 or myc-Hua1 retained the ability to mate, albeit at a slightly lower frequency (Figure S3E). Importantly, overexpressing Rsp5 suppressed the effect Ub-Hua1 overexpression, greatly diminishing the residual rate of mating following a shift into dextrose (Figure 5D). To determine if the potency of Ub-Hua1 as an Rsp5 competitor was mediated through the N-lobe UBS of the Rsp5-HECT domain, we compared the effects of Hua1 and Ub-Hua1 overexpression in wild-type cells and cells carrying the Rsp5 $F_{618}A$ mutation (*rsp5*$^{\Delta Ub}$, Figure 4) that neutralizes the N-lobe UBS [23]. As reported earlier, the *rsp5*$^{\Delta Ub}$ mutant is less active overall [23], therefore myc-Hua1 overexpression is sufficient to compromise growth at 37°C whereas Hua1$^{\Delta N}$ had no effect (Figure 5E). Importantly, unlike wild-type cells, the *rsp5*$^{\Delta Ub}$ mutant showed no difference in the level of growth inhibition by myc-Hua1 vs myc-Ub-Hua1, supporting the model that the effect of ubiquitinated-adaptors is mediated through the N-lobe UBS (Figure 4). The model further predicts that ubiquitinated adaptors associate better with Rsp5. Co-immunoprecipitation experiments using lysates from yeast expressing the myc-Hua1 variants showed that Rsp5 associated with both Hua1 and Ub-Hua1, yet that association was greatly diminished for Hua1$^{\Delta N}$, lacking its canonical PY motif and N-terminal ubiquitination sites (Figure 5F, S3C). Importantly, the proportion of Rsp5 co-immunoprecipitated with myc-Ub-Hua1 was far higher than for myc-Hua1, indicating that Ub-Hua1 binds Rsp5 better than Hua1 alone. This was confirmed through *in vitro* binding studies wherein Hua1 and Ub-Hua1 were fused to the *streptococcal* protein G as a solubility tag and the HA epitope for immuno-detection and produced in bacteria. Lysates were mixed and allowed to bind beads coated with maltose-binding protein (MBP) or MBP fused to full-length Rsp5. Immunoblotting fractions revealed that Ub-Hua1 bound with much higher efficiency to MBP-Rsp5 than Hua1 (Figure 5G). Finally, immunoprecipitation experiments using cells carrying WT *RSP5* or mutant *rsp5*$^{\Delta Ub}$ allele as their sole copy showed that the binding of Ub-Hua1 to Rsp5 relies on an intact UBS, as significantly less Ub-Hua1 was recovered from cells expressing the *rsp5*$^{\Delta Ub}$ ($F_{618}A$) allele (Figure S3D).

The deubiquitinating enzyme Ubp2 regulates adaptor protein activity

Rsp5 forms a complex with the deubiquitinating enzyme Ubp2 via Rup1, and loss of Ubp2 compromises many Rsp5-dependent functions [13, 18, 20, 21]. Under the proposed model, one function of Ubp2 could be to deubiquitinate Rsp5 adaptors, facilitating their ability to disengage Rsp5 and allow for exchange of new adaptors. This model would predict loss of Ubp2 inhibits adaptor exchange and diminishes the pool of ‘free’ Rsp5 available for adaptor engagement, resulting in failure to ubiquitinate the full repertoire of substrates (Figure 4).

Ubp2 associates with Rsp5 via the linker protein Rup1 (Figure 6A), this association is not stoichiometric *in vivo*, however, since only a portion of these components are recovered by immunoprecipitation [20]. According to the model, *ubp2Δ* mutants would have no way of efficiently 'unlocking' ubiquitinated adaptors from Rsp5. More abundant adaptors would be converted to longer-lived stronger competitors that would compromise myriad Rsp5 functions and result in the plethora of defective Rsp5-dependent cargo sorting events previously observed [13, 20–22]. In this scenario, Hua1 would become a much more effective inhibitor, on par with the 'constitutively ubiquitinated' Ub-Hua1 fusion protein, since it would remain ubiquitinated once bound to Rsp5. Indeed, we found that the inhibitory effect of Hua1 and Ub-Hua1 were very similar in *ubp2Δ* and *ubp2Δ rup1Δ* mutants as measured in growth assays at 37°C (Figure 6B), in contrast to the differential effects of Hua1 compared with Ub-Hua1 overexpression observed in WT cells. In addition, Hua1 and Ub-Hua1 were equally potent at inhibiting MVB sorting of Mup1-GFP into the vacuole of *ubp2Δ* cells, whereas in WT cells, only Ub-Hua1 could inhibit sorting of Mup1-GFP (Figure 6C, S4A). The idea that Rsp5 is ineffective in *ubp2*Δ mutants because it is locked into ubiquitinated complexes that sequester its ability cycle amongst a variety of adaptors was supported by Rsp5 overexpression experiments. Here, we found that overexpressing Rsp5 corrected the sorting defects of GFP-Cps1 in *ubp2Δ* mutants (Figure 6D). We also found that WT and *ubp2Δ* cells had similar levels of myc*-Hua1 and myc*-Hua1$^{K>R}$ (Figure 6E, S4B), supporting the hypothesis that Ubp2 does not promote Rsp5 processes in the cell solely by elevating levels of Rsp5 adaptor proteins.

To fully test the model, we assessed whether Rsp5-dependent endocytosis of Mup1 was promoted or inhibited by cognate and non-cognate Rsp5 adaptor proteins in WT and *ubp2Δ* cells (Figure 7A). In WT cells, as described above, overexpressing Art1 was sufficient to drive Mup1-GFP into endosomes in the absence of methionine. Downregulation was more profound in WT cells expressing Art1-Ub, where the majority Mup1-GFP was found within the vacuole lumen. In *ubp2*Δ cells, the degree of Mup1 downregulation was extensive for both Art1 and Art1-Ub overexpression, suggesting that in the absence of Ubp2, Art1 functions as strongly as a 'constitutively ubiquitinated' version (Figure 7B, 7C, S4C). Other Rsp5 adaptors, for which Mup1 is a non-cognate substrate and would therefore compete with Art1 for Rsp5-dependent downregulation of Mup1, behaved with the same profile. In WT cells, addition of methionine caused efficient sorting of Mup1 from the cell surface to the vacuolar lumen. However, overexpressing myc-Ub-Hua1 or Rim8-V5-Ub antagonized Mup1 sorting to the vacuole, causing a portion Mup1-GFP to persist at the cell surface (Figure 7C, 7D). Inhibition of methionine-stimulated downregulation of Mup1-GFP was not observed by overexpressing myc-Hua1 or Rim8-V5 that were not fused to Ub, consistent with the preceding experiments showing that 'constitutively ubiquitinated' forms of Rsp5 adaptors are stronger competitive inhibitors than their natural counterparts. Importantly, in *ubp2*Δ cells, the wild-type forms of Hua1 and Rim8 were just as inhibitory as their Ub-fused counterparts. Inhibition of Mup1-GFP downregulation was not observed when overexpressing either Hua1$^{\Delta N}$ nor Rim8$^{K>R}$, suggesting that Hua1 and Rim8 become strong inhibitors in *ubp2Δ* null cells because the pool bound to Rsp5 is more persistently ubiquitinated.

DISCUSSION

Rsp5 can either directly bind substrates or use a variety of adaptor proteins to facilitate substrate ubiquitination [5, 7, 9–11]. Rsp5 adaptors also undergo ubiquitination, and for some such as Art1, Rod1, Csr2, and as shown here for Hua1, ubiquitination is required for them to achieve their full function [9, 16, 31]. We find that adaptor ubiquitination enhances activity towards cognate substrates whilst also inhibiting ubiquitination of non-cognate substrates, supporting a model in which ubiquitinated adaptors better compete for occupancy on Rsp5. In some cases, such as Art1, translational fusion of Ub greatly potentiates activity towards its cognate substrates such as Mup1, which is downregulated even in the absence of its substrate methionine. In all cases examined here, attachment of Ub onto adaptors potentiated their ability to disrupt Rsp5-dependent regulation of non-cognate substrates, likely reflecting their enhanced ability to co-opt a limited pool of Rsp5. Previous studies have also provided evidence for competition amongst Rsp5 adaptors. For instance, overexpressing Sna3, Ssh4, or Ear1 inhibits Rsp5-dependent downregulation of Tat2 for which Art1 and Art2 serve as cognate adaptors [10, 11, 33, 38, 39]. Additionally, overexpressing the Aly1, Aly2, or Ssh4 adaptor proteins blocks Rsp5-dependent endocytosis of Gap1, for which Bul1 and Bul2 serve as cognate adaptors [34, 38, 42]. Moreover, deletion of Bul2 potentiates the ability of Bsd2 to downregulate Smf1 and deletion of Bul1 allows for better downregulation of Can1 [43]. Our studies indicate that ubiquitinated versions of adaptors compete better, providing an explanation for how ubiquitination appears to ‘activate’ adaptors and potentiate their activity. This model is further supported by our observations that artificially ubiquitinated Hua1 binds Rsp5 better *in vitro* and *in vivo*, providing a biochemical correlate for how ubiquitinated adaptors might better direct Rsp5 to their cognate substrates while also depriving other adaptors from occupancy on Rsp5 (Figure 5).

Translational fusion of ubiquitin converted adaptors into potent competitors, but there may be additional conformational criteria to convert an adaptor into a form that can work more potently on its cognate substrates. Art1, Rim8, and Hua1 undergo site-specific ubiquitination, and these particular sites may be required in some contexts to form a specific quaternary structure with Rsp5 and their substrate. This may explain why activity of the $Rim8^{K>R}$ mutant towards its cognate substrate within the Rim101 pathway was not restored upon Ub-fusion (Figure 3). Overall, our data for Rim8 are largely consistent with previous studies that demonstrate a role for ubiquitination of Rim8, which have yielded seemingly disparate results. In *Aspergillus*, the PalF/Rim8 Rsp5 adaptor is required for processing of PacC/Rim101 in response to a shift to alkaline pH. Overexpressing a translational PalF-Ub fusion protein causes promiscuous pH-independent activation of the PacC/Rim101 whereas PalF expression alone does not [30]. In *Saccharomyces cerevisiae*, however, a $Rim8^{K521R}$ mutant still supports pH-dependent activation of the Rim101 pathway [17]. We found that overexpressing Rim8, whether it was fused to Ub or not, caused the promiscuous pH-independent activation of the Rim101 pathway, suggesting that the threshold for activating the RIM101 pathway may be low in the strains we tested (Figure 3F). This effect was dependent on Rim8 ubiquitination since overexpressing the $Rim8^{K521R}$ mutant had no effect. These data combined with the observation that fusion of Ub onto Rim8 elicited a

stronger inhibitory effect on non-cognate substrates such as Mup1-GFP aligns again with the idea that ubiquitination of Rim8 potentiates its ability to direct Rsp5 towards activating the Rim101 pathway but that these enhancing effects are not strictly required in *S. cerevisiae* laboratory strains, possibly due to a sensitized system.

We propose that the sensor that responds to adaptor ubiquitination is Rsp5 itself, via the Ub-binding surface (UBS) within the N-lobe of the HECT catalytic domain [23–25]. Inactivating this surface abolished the advantage that Ub-Hua1 had over Hua1 in causing dominant-negative effects on Rsp5 function and decreased association with Rsp5 in immunoprecipitation experiments (Figure 5, S3C). These data suggest a mechanism whereby the Rsp5 UBS provides an additional interface to help 'lock on' adaptors that also connect with Rsp5 WW domains via their PY motifs. An analogous dual-site binding effect has also been observed between Smurf2 and its substrate RhoA, which binds better to the Smurf2 HECT domain when presented as a Ub-fusion protein [26]. The Rsp5 Ub-binding surface may also play additional stimulatory roles *in vivo*. Analysis of Rsp5 and other Nedd4-family members *in vitro* shows that the UBS is important for polyubiquitin chain elongation, with a minor role in the initial mono-ubiquitination of substrate [24–26]. Although mono-ubiquitination of plasma membrane cargoes is sufficient for their MVB sorting and downregulation [44], any loss of the ability to elaborate a longer K_{63} chain, that would have more avid binding to Ub-sorting receptors, would likely compromise the ability of Rsp5 to downregulate membrane protein cargoes. One speculation is that the occupancy of the Ub-binding surface by a ubiquitinated adaptor protein may constrain the activity of the Rsp5-UBS resulting in the addition of mono-Ub and short K63-linked chains on membrane protein substrates. Whereas in other contexts, such as ubiquitination of heat damaged cytosolic proteins, the Rsp5-UBS might be unfettered and potentiate formation of longer chains that include K48 linkages [28, 40]. Aside from these two potential stimulatory activities for the UBS, an inhibitory role has also been proposed [45]. In this instance, the UBS binds to autoubiquitinated Rsp5, creating an oligomer that is less active *in vitro*. Since eliminating the Rsp5 UBS itself clearly inhibits Rsp5 activity *in vivo* rather than stimulate it by eliminating a sole inhibitory function, it will be interesting to determine how these potential stimulatory and inhibitory mechanisms coordinate with one another physiologically.

Overall, this model specifies a process whereby adaptors constantly compete with each other for occupancy with Rsp5. Upon binding, they can undergo ubiquitination and occupy Rsp5 more efficiently. The model also explains how Rsp5 association with the deubiquitinating enzyme Ubp2 can promote Rsp5 activity in general. Ubp2 clearly antagonizes Rsp5 activity *in vitro* and can also oppose Rsp5 activity on some substrates *in vivo* [13, 18, 19]. Yet how Ubp2 plays a stimulatory role in promoting the downregulation and MVB sorting of numerous membrane proteins as well as degradation of cytosolic proteins is difficult to reconcile with a simple view of this relationship [20, 21, 46]. One potential mechanism is that Ubp2 antagonizes Rsp5-dependent ubiquitination, protecting adaptors or Rsp5 itself from proteosomal degradation [47]. Yet, Rsp5 levels are not lower in *ubp2Δ* mutants [18] and triggering the pathways that use various adaptors such as Bul1, Bul2, Rim8, and Aly2 results in the generation of stably mono-ubiquitinated forms of the adaptors rather than generating intermediates for accelerated degradation [14, 15, 17]. Moreover, this does not

explain how overexpressing Rsp5 in *ubp2*Δ cells can suppress the inhibitory effects on downregulation of membrane proteins (Figure 6D), since Rsp5 overexpression should exacerbate the destruction of adaptor proteins. Additionally, we see no changes in the levels of Hua1 or Hua1$^{K>R}$ in wild-type vs *ubp2*Δ mutants (Figure 6E). Rather, we propose that a critical function of Ubp2 is to remove Ub from ubiquitinated adaptor proteins allowing them to cycle off Rsp5 more readily. Thus, in the absence of Ubp2, the availability of Rsp5 for a wide range of adaptors would be restricted because the subset of ubiquitinated adaptors bound to Rsp5 would compete away the larger pool of adaptors more strongly. The prediction from this model is that the ability to compete for limited Rsp5 in *ubp2*Δ cells would show little difference between adaptors-fused to Ub that are resistant to deubiquitination versus wild-type adaptors that would be unable to undergo deubiquitination in the absence of Ubp2. This prediction was fulfilled in multiple experiments for both cognate and non-cognate substrates (Figs. 6, 7).

One of the implications from our observations and the model presented is that limited space on Rsp5 for its full set of adaptors and substrates enforces a level of coordinated regulation. This could impart a ‘zero-sum game’ scenario where stimulating ubiquitination of a particular set of substrates, by recruitment and activation of a subset of Rsp5 adaptors, necessarily diminishes the capability of other adaptors to access Rsp5 and direct its activity to their cognate substrates. Not only does this explain how one ligase can regulate so many distinct substrates under constantly changing metabolic conditions, but this mechanism could be especially potent when large sets of adaptors are under coordinated control, such as glucose responsive AMP-kinase, nitrogen responsive TORC1 and its downstream Npr1, or calcium signaling through calcineurin that could alter the broader landscape of multiple subsets Rsp5-dependent processes.

STAR METHODS

LEAD CONTACT AND MATERIALS AVAILABILITY

Further information and requests for resources and reagents should be directed to and will be fulfilled by the Lead Contact Robert Piper: robert-piper@uiowa.edu. All unique/stable reagents generated in this study are available from the Lead Contact without restriction.

EXPERIMENTAL MODEL AND SUBJECT DETAILS

Studies were conducted in haploid strains of Saccharomyces cerevisiae. Genotypes are described in Key Resource Table. Yeast cultures were grown in rich media (YPD: 2% glucose, 2% peptone, 1% yeast extract) or minimal media (Synthetic Complete (SC) 2% glucose, 1x yeast nitrogen base; Research Products International, Mount Prospect, IL) with amino acid and base drop out compositions (Formedium, Norfolk, UK) for plasmid selection. Cells carrying plasmids expressing proteins from the CUP1 promoter were grown in liquid or solid agar containing 50 μM copper chloride unless otherwise stated. Yeast transformation was performed using the Lithium acetate method [48].

METHOD DETAILS

Fluorescence microscopy—Yeast cultures expressing GFP tagged proteins were grown to mid-log phase (OD_{600} = 1.0), harvested and resuspended in “kill” buffer (100 mM Tris.HCl (pH 8.0), 0.2% (w/v) NaN_3 and NaF) prior to imaging with an epifluorescence microscope (BX60; Olympus) with a 100x objective lens with numerical aperture (NA) 1.4. Images were captured with a cooled charge-coupled device camera (Orca R2; Hamamatsu Photonics) using iVision-Mac software (Biovision Technology). Image processing for display was performed in Photoshop. Image processing for quantitation was performed with Fiji.

Viability assays—Prior to viability assays performed on solid agar media yeast cells were grown to mid-log phase in appropriate selection media lacking extra $CuCl_2$. OD_{600} measurements were used to harvest equivalent cell numbers from each culture, before cells were washed once with water and then diluted in a series of 10-fold dilution steps. 5–10μl of each dilution was then plated on SD media with and without $CuCl_2$ and grown at 30°C or 37°C and growth was subsequen tly recorded following 24–48 hr incubation.

Proteolytic processing of Rim101—Rim101 experiments were typically performed in SEY6210 cells, unless otherwise stated, as the processing upon pH shift was more obvious than in BY4742 cells (as shown in Figure S2A). Cells were transformed with the LEU2 marked plasmid pFL1 expressing 3xHA-Rim101 and co-transformed with either vector control or URA3 marked plasmids expressing either V5-Rim8 (and variants) as a cognate Rsp5 adaptor or myc-Hua1 (and variants) as a competing Rsp5 adaptor. Cells were grown to mid-log phase in SC-Ura-Leu media that was buffered to pH 5.5 with 50 mM MES (containing 50 μM $CuCl_2$ to induce expression of adaptors). Cell densities were estimated across samples using OD_{600} measurements, before harvesting equivalent cell numbers for each condition. Each sample was split into 3 equal tubes, pelleted and brought up in buffer of either 100 mM sodium citrate (pH = 3.5), 50 mM MES (pH = 5.5), or 50 mM MOPS (pH = 8.0) for 20 minutes before lysates were generated as described above. Samples were analysed by SDS-PAGE and immunoblotting with specific antibodies to appraise Rim101 species (anti-HA), levels of cognate Rim8 versions (anti-V5) and competing Hua1 versions (anti-myc), and loading controls (either anti-Rsp5 or anti-PGK)

Mating efficiency assay—Strain PLY4804 was created by replacing the endogenous STE3 promoter region of wild-type BY4742 cells with a Kanamycin resistance cassette followed by the GAL1 promoter and an N-terminal 3xHA epitope tag designed to replace the start methionine of the STE3 ORF. The strain was confirmed to express an HA-tagged version of Ste3 at the correct molecular weight when cells were grown in galactose (GAL) media, but expression was completely absent in the presence of dextrose (DEX). Importantly, the Mat**α** BY4742 GAL1–3xHA-STE3 carries the his3Δ mutation. This meant that successful mating with PLY42, a Mat**a** strain that carries wild-type HIS3 but is auxotrophic for histidine by virtue of the his4–519 mutation, could select for diploids in minimal media lacking histidine (SC-His). Mating reactions were first performed in cells growing in either glucose or galactose, with each strain grown to mid-log phase before 500μl of each being mixed and allowed to settled in a tube for 6 hours at 30°C in either GAL or

DEX containing rich media. At least 4 different dilutions of cell mixtures were then made and plated on SC-His plates and grown at 30 degrees for 48 hours. Colonies were counted from each dilution and used to estimate how many successful diploids were generated from each condition. This basic assay was then used to perform additional experiments, including a glucose repression 'pulse chase' of Ste3 where GAL grown cells were split into two and incubated with either DEX or GAL for 20 minutes prior to the mating assay as described. This pulse chase experiment was then performed in minimal media in cells expressing URA3 borne Hua1 constructs, grown in the presence of 50 μM $CuCl_2$ or cells expressing Ub-Hua1 with either HA-Rsp5 or a vector control. Average His^+ diploids for each experimental condition were calculated with the standard deviation shown with error bars.

Immunoprecipitation & Immunodetection—For whole-cell lysates, yeast cells were pelleted and first resuspended in 0.2 N NaOH for two minutes. Laemmli sample buffer containing 8 M urea was added (75 mM Tris [pH 6.8], 8 M urea, 3% SDS with bromophenol blue), and lysates resolved by SDS-PAGE, transferred to nitrocellulose, and analysed by blotting with the indicated antibodies. For co-immunoprecipitation experiments cells transformed with copper inducible myc-tagged Hua1 constructs. Cells were grown to mid-log phase in 25 μM CuCl2, harvested, washed and resuspended in lysis buffer (PBS and protease inhibitor cocktail) and lysed using the One-shot instrument from Constant Systems, Ltd.. Cell debris was removed by centrifugation and the supernatant ('Input') incubated with polyclonal goat anti-myc antibodies conjugated to sepharose for 90 min on ice. After washing 3 times with lysis buffer containing 0.1% Tween-20, bound proteins were eluted from the beads using Laemmli sample buffer, followed by standard immunoblotting procedures (described above) using anti-HA and anti-myc monoclonal antibodies. Antibodies and antibody-based reagents are further described in the key resource table.

Isolation of ubiquitinated proteins—Strain PLY4272 was optimized for purification of ubiquitinated proteins by replacing the UBI4 gene with a His6 tagged version of Ubiquitin, separated by a short 8 amino acid linker (ALINQERA) and expressed from a low level constitutive promoter (a mutant form of the TEF1 promoter (Nevoigt et al., 2006). Hbt1 is a significant contaminant to His6-tag purifications from yeast cell lysates (MacDonald et al., 2017), so the chromosomal HBT1 ORF was modified to truncate the C terminus encoding a histidine rich region (amino acids 967–1049). PLY4272 also lacks the PDR5 gene. A large (2 Litre) culture of PLY4272 cells was prepared from single colony transformants expressing either HA-tagged Hua1, myc-Hua1, Art1-HA and Rim8-V5 were grown to mid-log phase, harvested, treated for 3 min with 0.2 N NaOH prior to lysates being generated in denaturing buffer containing 2.5% SDS and 8 M urea. Cells were then diluted 20-fold in binding buffer (50 mM Tris.HCl pH 8.0, 8 M urea, 10% (w/v) glycerol, 5 mM β-Me), incubated for 2 hrs at room temperature with 3 ml (50% slurry) Ni^{2+}-NTA agarose and collected in a column. Beads were washed with 10 x with binding buffer containing 10 mM imidazole and bound proteins eluted using 10ml binding buffer with pH shifted to 4.5. These eluates were rebound to a small volume of (300–400 μl) 50% slurry Ni^{2+}-NTA agarose for a further 2 hrs at room temperature. Beads were then harvested in a column and washed 10 x with binding buffer containing 10 mM imidazole and then eluted in 1 ml buffer containing 350 mM imidazole. Original lysates and purified eluates containing ubiquitinated proteins were

resuspended in Laemmli sample buffer [49], resolved by SDS-PAGE, transferred to nitrocellulose and immunoblotted with antibodies raised against the specific epitope of each fusion protein, as described above.

QUANTIFICATION AND STATISTICAL ANALYSIS

To quantify the percentage of Mup1-GFP at the cell surface, matched DIC and green fluorescence images were aligned using the Registration/Align function within Fiji [50]. Segmentation was performed on the DIC image using the Cell Magic Wand plugin (Min = 8, Max = 300, roughness = 2.0) to define a region of interest for the whole cell (R1) to which a negative expansion was applied to achieve a morphological transformation for a smaller region of interest lacking signal from the plasma membrane (R2). Following background subtraction, the percentage Mup1-GFP at the surface was given by R1-R2/R1*100. A series of smaller regions of interest were generated by sequential negative expansions, and the lowest mean intensity value across this set was taken as the level of background. To quantify the overall distribution localization profiles, cells were scored qualitatively for either having fluorescence exclusively, partially, or not detectable at the cell surface and whether fluorescence was found exclusively or partially within endosomal puncta or vacuole lumens. Percentage of cells that fit these profiles was calculated and presented as a binned dataset.

DATA CODE AND AVAILABILITY

The published article includes all data generated or analyzed during this study with the exception of raw micrographs analysed for Figures 6 and 7.

Data for quantitation in Figures 6 and 7 have not been deposited in a public repository because they were too numerous and exemplified in representative micrographs and presented in graphed format. They are available from the lead contact on request.

Supplementary Material

Refer to Web version on PubMed Central for supplementary material.

ACKNOWLEDGEMENTS

We thank members of the laboratory for constructs, advice and helpful discussions, as well as L. Hicke for the generous gift of yeast strains. This work was supported by AHA post-doctoral fellowship award 13POST 14710042 to CM and a fellowship through the NIH Institutional Training grant 5T32DK007690-19 to SBS and NIH RO1GM058202 to RCP.

REFERENCES

1. Rotin D, and Kumar S (2009). Physiological functions of the HECT family of ubiquitin ligases. Nat Rev Mol Cell Biol 10, 398–409. [PubMed: 19436320]
2. Piper RC, Dikic I, and Lukacs GL (2014). Ubiquitin-dependent sorting in endocytosis. Cold Spring Harbor perspectives in biology 6.
3. Lu K, Yin X, Weng T, Xi S, Li L, Xing G, Cheng X, Yang X, Zhang L, and He F (2008). Targeting WW domains linker of HECT-type ubiquitin ligase Smurf1 for activation by CKIP-1. Nat Cell Biol 10, 994–1002. [PubMed: 18641638]
4. Lauwers E, Erpapazoglou Z, Haguenauer-Tsapis R, and Andre B (2010). The ubiquitin code of yeast permease trafficking. Trends Cell Biol 20, 196–204. [PubMed: 20138522]

5. Leon S, and Haguenauer-Tsapis R (2009). Ubiquitin ligase adaptors: regulators of ubiquitylation and endocytosis of plasma membrane proteins. Exp Cell Res 315, 1574–1583. [PubMed: 19070615]
6. Shearwin-Whyatt L, Dalton HE, Foot N, and Kumar S (2006). Regulation of functional diversity within the Nedd4 family by accessory and adaptor proteins. Bioessays 28, 617–628. [PubMed: 16700065]
7. Hettema EH, Valdez-Taubas J, and Pelham HR (2004). Bsd2 binds the ubiquitin ligase Rsp5 and mediates the ubiquitination of transmembrane proteins. EMBO J 23, 1279–1288. [PubMed: 14988731]
8. Leon S, Erpapazoglou Z, and Haguenauer-Tsapis R (2008). Ear1p and Ssh4p are new adaptors of the ubiquitin ligase Rsp5p for cargo ubiquitylation and sorting at multivesicular bodies. Mol Biol Cell 19, 2379–2388. [PubMed: 18367543]
9. Lin CH, MacGurn JA, Chu T, Stefan CJ, and Emr SD (2008). Arrestin-related ubiquitin-ligase adaptors regulate endocytosis and protein turnover at the cell surface. Cell 135, 714–725. [PubMed: 18976803]
10. MacDonald C, Stringer DK, and Piper RC (2012). Sna3 Is an Rsp5 Adaptor Protein that Relies on Ubiquitination for Its MVB Sorting. Traffic.
11. Nikko E, and Pelham HR (2009). Arrestin-mediated endocytosis of yeast plasma membrane transporters. Traffic 10, 1856–1867. [PubMed: 19912579]
12. Nikko E, Sullivan JA, and Pelham HR (2008). Arrestin-like proteins mediate ubiquitination and endocytosis of the yeast metal transporter Smf1. EMBO Rep 9, 1216–1221. [PubMed: 18953286]
13. Kee Y, Munoz W, Lyon N, and Huibregtse JM (2006). The deubiquitinating enzyme Ubp2 modulates Rsp5-dependent Lys63-linked polyubiquitin conjugates in Saccharomyces cerevisiae. J Biol Chem 281, 36724–36731. [PubMed: 17028178]
14. Merhi A, and Andre B (2012). Internal amino acids promote Gap1 permease ubiquitylation via TORC1/Npr1/14–3-3-dependent control of the Bul arrestin-like adaptors. Mol Cell Biol 32, 4510–4522. [PubMed: 22966204]
15. Hatakeyama R, Kamiya M, Takahara T, and Maeda T (2010). Endocytosis of the aspartic acid/glutamic acid transporter Dip5 is triggered by substrate-dependent recruitment of the Rsp5 ubiquitin ligase via the arrestin-like protein Aly2. Mol Cell Biol 30, 5598–5607. [PubMed: 20956561]
16. Becuwe M, Vieira N, Lara D, Gomes-Rezende J, Soares-Cunha C, Casal M, Haguenauer-Tsapis R, Vincent O, Paiva S, and Leon S (2012). A molecular switch on an arrestin-like protein relays glucose signaling to transporter endocytosis. J Cell Biol 196, 247–259. [PubMed: 22249293]
17. Herrador A, Herranz S, Lara D, and Vincent O (2010). Recruitment of the ESCRT machinery to a putative seven-transmembrane-domain receptor is mediated by an arrestin-related protein. Mol Cell Biol 30, 897–907. [PubMed: 20028738]
18. Kee Y, Lyon N, and Huibregtse JM (2005). The Rsp5 ubiquitin ligase is coupled to and antagonized by the Ubp2 deubiquitinating enzyme. EMBO J 24, 2414–2424. [PubMed: 15933713]
19. Lam MH, and Emili A (2013). Ubp2 regulates Rsp5 ubiquitination activity in vivo and in vitro. PLoS One 8, e75372. [PubMed: 24069405]
20. Lam MH, Urban-Grimal D, Bugnicourt A, Greenblatt JF, Haguenauer-Tsapis R, and Emili A (2009). Interaction of the deubiquitinating enzyme Ubp2 and the e3 ligase Rsp5 is required for transporter/receptor sorting in the multivesicular body pathway. PLoS One 4, e4259. [PubMed: 19165343]
21. Ren J, Kee Y, Huibregtse JM, and Piper RC (2007). Hse1, a component of the yeast Hrs-STAM ubiquitin-sorting complex, associates with ubiquitin peptidases and a ligase to control sorting efficiency into multivesicular bodies. Mol Biol Cell 18, 324–335. [PubMed: 17079730]
22. Erpapazoglou Z, Dhaoui M, Pantazopoulou M, Giordano F, Mari M, Leon S, Raposo G, Reggiori F, and Haguenauer-Tsapis R (2012). A dual role for K63-linked ubiquitin chains in multivesicular body biogenesis and cargo sorting. Mol Biol Cell 23, 2170–2183. [PubMed: 22493318]
23. French ME, Kretzmann BR, and Hicke L (2009). Regulation of the RSP5 ubiquitin ligase by an intrinsic ubiquitin-binding site. J Biol Chem 284, 12071–12079. [PubMed: 19252184]
24. Kim HC, Steffen AM, Oldham ML, Chen J, and Huibregtse JM (2011). Structure and function of a HECT domain ubiquitin-binding site. EMBO Rep 12, 334–341. [PubMed: 21399621]

25. Maspero E, Mari S, Valentini E, Musacchio A, Fish A, Pasqualato S, and Polo S (2011). Structure of the HECT:ubiquitin complex and its role in ubiquitin chain elongation. EMBO Rep 12, 342–349. [PubMed: 21399620]
26. Ogunjimi AA, Wiesner S, Briant DJ, Varelas X, Sicheri F, Forman-Kay J, and Wrana JL (2010). The ubiquitin binding region of the Smurf HECT domain facilitates polyubiquitylation and binding of ubiquitylated substrates. J Biol Chem 285, 6308–6315. [PubMed: 20026602]
27. Lee JR, Oestreich AJ, Payne JA, Gunawan MS, Norgan AP, and Katzmann DJ (2009). The HECT domain of the ubiquitin ligase Rsp5 contributes to substrate recognition. J Biol Chem 284, 32126–32137. [PubMed: 19744925]
28. Fang NN, Chan GT, Zhu M, Comyn SA, Persaud A, Deshaies RJ, Rotin D, Gsponer J, and Mayor T (2014). Rsp5/Nedd4 is the main ubiquitin ligase that targets cytosolic misfolded proteins following heat stress. Nat Cell Biol 16, 1227–1237. [PubMed: 25344756]
29. Peng J, Schwartz D, Elias JE, Thoreen CC, Cheng D, Marsischky G, Roelofs J, Finley D, and Gygi SP (2003). A proteomics approach to understanding protein ubiquitination. Nature biotechnology 21, 921–926.
30. Hervas-Aguilar A, Galindo A, and Penalva MA (2010). Receptor-independent Ambient pH signaling by ubiquitin attachment to fungal arrestin-like PalF. J Biol Chem 285, 18095–18102. [PubMed: 20368671]
31. Hovsepian J, Defenouillere Q, Albanese V, Vachova L, Garcia C, Palkova Z, and Leon S (2017). Multilevel regulation of an alpha-arrestin by glucose depletion controls hexose transporter endocytosis. J Cell Biol 216, 1811–1831. [PubMed: 28468835]
32. Herrador A, Leon S, Haguenauer-Tsapis R, and Vincent O (2013). A mechanism for protein monoubiquitination dependent on a trans-acting ubiquitin-binding domain. J Biol Chem 288, 16206–16211. [PubMed: 23645667]
33. Hiraki T, and Abe F (2010). Overexpression of Sna3 stabilizes tryptophan permease Tat2, potentially competing for the WW domain of Rsp5 ubiquitin ligase with its binding protein Bul1. FEBS Lett 584, 55–60. [PubMed: 19944104]
34. O'Donnell AF, Apffel A, Gardner RG, and Cyert MS (2010). Alpha-arrestins Aly1 and Aly2 regulate intracellular trafficking in response to nutrient signaling. Mol Biol Cell 21, 3552–3566. [PubMed: 20739461]
35. MacDonald C, Stringer DK, and Piper RC (2012). Sna3 is an Rsp5 adaptor protein that relies on ubiquitination for its MVB sorting. Traffic 13, 586–598. [PubMed: 22212814]
36. Reggiori F, and Pelham HR (2001). Sorting of proteins into multivesicular bodies: ubiquitin-dependent and -independent targeting. EMBO J 20, 5176–5186. [PubMed: 11566881]
37. Penalva MA, Lucena-Agell D, and Arst HN Jr. (2014). Liaison alcaline: Pals entice non-endosomal ESCRTs to the plasma membrane for pH signaling. Curr Opin Microbiol 22, 49–59. [PubMed: 25460796]
38. Kota J, Melin-Larsson M, Ljungdahl PO, and Forsberg H (2007). Ssh4, Rcr2 and Rcr1 affect plasma membrane transporter activity in Saccharomyces cerevisiae. Genetics 175, 1681–1694. [PubMed: 17287526]
39. Hiraki T, Usui K, and Abe F (2010). Overexpression of EAR1 and SSH4 that encode PPxY proteins in the multivesicular body provides stability to tryptophan permease Tat2, allowing yeast cells to grow under high hydrostatic pressure. High Pressure Research 30, 514–518.
40. French ME, Klosowiak JL, Aslanian A, Reed SI, Yates JR 3rd, and Hunter T (2017). Mechanism of ubiquitin chain synthesis employed by a HECT domain ubiquitin ligase. J Biol Chem 292, 10398–10413. [PubMed: 28461335]
41. Davis NG, Horecka JL, and Sprague GF Jr. (1993). Cis- and trans-acting functions required for endocytosis of the yeast pheromone receptors. J Cell Biol 122, 53–65. [PubMed: 8391002]
42. Helliwell SB, Losko S, and Kaiser CA (2001). Components of a ubiquitin ligase complex specify polyubiquitination and intracellular trafficking of the general amino acid permease. J Cell Biol 153, 649–662. [PubMed: 11352928]
43. Novoselova TV, Zahira K, Rose RS, and Sullivan JA (2012). Bul proteins, a nonredundant, antagonistic family of ubiquitin ligase regulatory proteins. Eukaryot Cell 11, 463–470. [PubMed: 22307975]

44. Stringer DK, and Piper RC (2011). A single ubiquitin is sufficient for cargo protein entry into MVBs in the absence of ESCRT ubiquitination. J Cell Biol 192, 229–242. [PubMed: 21242292]
45. Attali I, Tobelaim WS, Persaud A, Motamedchaboki K, Simpson-Lavy KJ, Mashahreh B, Levin-Kravets O, Keren-Kaplan T, Pilzer I, Kupiec M, et al. (2017). Ubiquitylation-dependent oligomerization regulates activity of Nedd4 ligases. EMBO J 36, 425–440. [PubMed: 28069708]
46. Fang NN, Zhu M, Rose A, Wu KP, and Mayor T (2016). Deubiquitinase activity is required for the proteasomal degradation of misfolded cytosolic proteins upon heat-stress. Nat Commun 7, 12907. [PubMed: 27698423]
47. Ho HC, MacGurn JA, and Emr SD (2017). Deubiquitinating enzymes Ubp2 and Ubp15 regulate endocytosis by limiting ubiquitination and degradation of ARTs. Mol Biol Cell 28, 1271–1283. [PubMed: 28298493]
48. Gietz RD, Schiestl RH, Willems AR, and Woods RA (1995). Studies on the transformation of intact yeast cells by the LiAc/SS-DNA/PEG procedure. Yeast 11, 355–360. [PubMed: 7785336]
49. Laemmli UK (1970). Cleavage of structural proteins during the assembly of the head of bacteriophage T4. Nature 227, 680–685. [PubMed: 5432063]
50. Schindelin J, Arganda-Carreras I, Frise E, Kaynig V, Longair M, Pietzsch T, Preibisch S, Rueden C, Saalfeld S, Schmid B, et al. (2012). Fiji: an open-source platform for biological-image analysis. Nat Methods 9, 676–682. [PubMed: 22743772]
51. Stamenova SD, Dunn R, Adler AS, and Hicke L (2004). The Rsp5 ubiquitin ligase binds to and ubiquitinates members of the yeast CIN85-endophilin complex, Sla1-Rvs167. J Biol Chem 279, 16017–16025. [PubMed: 14761940]
52. Richardson SC, Winistorfer SC, Poupon V, Luzio JP, and Piper RC (2004). Mammalian late vacuole protein sorting orthologues participate in early endosomal fusion and interact with the cytoskeleton. Mol Biol Cell 15, 1197–1210. [PubMed: 14668490]
53. Casadaban MJ, and Cohen SN (1980). Analysis of gene control signals by DNA fusion and cloning in Escherichia coli. J Mol Biol 138, 179–207. [PubMed: 6997493]
54. Brachmann CB, Davies A, Cost GJ, Caputo E, Li J, Hieter P, and Boeke JD (1998). Designer deletion strains derived from Saccharomyces cerevisiae S288C: a useful set of strains and plasmids for PCR-mediated gene disruption and other applications. Yeast 14, 115–132. [PubMed: 9483801]
55. Robinson JS, Klionsky DJ, Banta LM, and Emr SD (1988). Protein sorting in Saccharomyces cerevisiae: isolation of mutants defective in the delivery and processing of multiple vacuolar hydrolases. Mol Cell Biol 8, 4936–4948. [PubMed: 3062374]
56. MacDonald C, Winistorfer S, Pope RM, Wright ME, and Piper RC (2017). Enzyme reversal to explore the function of yeast E3 ubiquitin-ligases. Traffic 18, 465–484. [PubMed: 28382714]
57. MacDonald C, Buchkovich NJ, Stringer DK, Emr SD, and Piper RC (2012). Cargo ubiquitination is essential for multivesicular body intralumenal vesicle formation. EMBO Rep 13, 331–338. [PubMed: 22370727]
58. Rothman JH, Howald I, and Stevens TH (1989). Characterization of genes required for protein sorting and vacuolar function in the yeast Saccharomyces cerevisiae. EMBO J 8, 2057–2065. [PubMed: 2676511]
59. Dunn R, and Hicke L (2001). Domains of the Rsp5 ubiquitin-protein ligase required for receptor-mediated and fluid-phase endocytosis. Mol Biol Cell 12, 421–435. [PubMed: 11179425]
60. Gerhard W, Yewdell J, Frankel ME, and Webster R (1981). Antigenic structure of influenza virus haemagglutinin defined by hybridoma antibodies. Nature 290, 713–717. [PubMed: 6163993]
61. Evan GI, Lewis GK, Ramsay G, and Bishop JM (1985). Isolation of monoclonal antibodies specific for human c-myc proto-oncogene product. Mol Cell Biol 5, 3610–3616. [PubMed: 3915782]
62. Golnik R, Lehmann A, Kloetzel PM, and Ebstein F (2016). Major Histocompatibility Complex (MHC) Class I Processing of the NY-ESO-1 Antigen Is Regulated by Rpn10 and Rpn13 Proteins and Immunoproteasomes following Non-lysine Ubiquitination. J Biol Chem 291, 8805–8815. [PubMed: 26903513]
63. Christensen ND, Dillner J, Eklund C, Carter JJ, Wipf GC, Reed CA, Cladel NM, and Galloway DA (1996). Surface conformational and linear epitopes on HPV-16 and HPV-18 L1 virus-like particles as defined by monoclonal antibodies. Virology 223, 174–184. [PubMed: 8806551]

64. Crowe J, Dobeli H, Gentz R, Hochuli E, Stuber D, and Henco K (1994). 6xHis-Ni-NTA chromatography as a superior technique in recombinant protein expression/purification. Methods Mol Biol 31, 371–387. [PubMed: 7921034]

65. Sikorski RS, and Hieter P (1989). A system of shuttle vectors and yeast host strains designed for efficient manipulation of DNA in Saccharomyces cerevisiae. Genetics 122, 19–27. [PubMed: 2659436]

66. Odorizzi G, Babst M, and Emr SD (1998). Fab1p PtdIns(3)P 5-kinase function essential for protein sorting in the multivesicular body. Cell 95, 847–858. [PubMed: 9865702]

67. Urbanowski JL, and Piper RC (1999). The iron transporter Fth1p forms a complex with the Fet5 iron oxidase and resides on the vacuolar membrane. J Biol Chem 274, 38061–38070. [PubMed: 10608875]

68. Hayashi M, Fukuzawa T, Sorimachi H, and Maeda T (2005). Constitutive activation of the pH-responsive Rim101 pathway in yeast mutants defective in late steps of the MVB/ESCRT pathway. Mol Cell Biol 25, 9478–9490. [PubMed: 16227598]

69. Gajewska B, Kaminska J, Jesionowska A, Martin NC, Hopper AK, and Zoladek T (2001). WW domains of Rsp5p define different functions: determination of roles in fluid phase and uracil permease endocytosis in Saccharomyces cerevisiae. Genetics 157, 91–101. [PubMed: 11139494]

HIGHLIGHTS

- The Rsp5 substrate adaptor protein Hua1 requires ubiquitination to function
- Rsp5 adaptor proteins compete for Rsp5 function more potently when ubiquitinated
- Elevated function of ubiquitinated adaptors depends on a Ub-binding site on Rsp5
- Ubp2 activity may unlock ubiquitinated adaptors from Rsp5

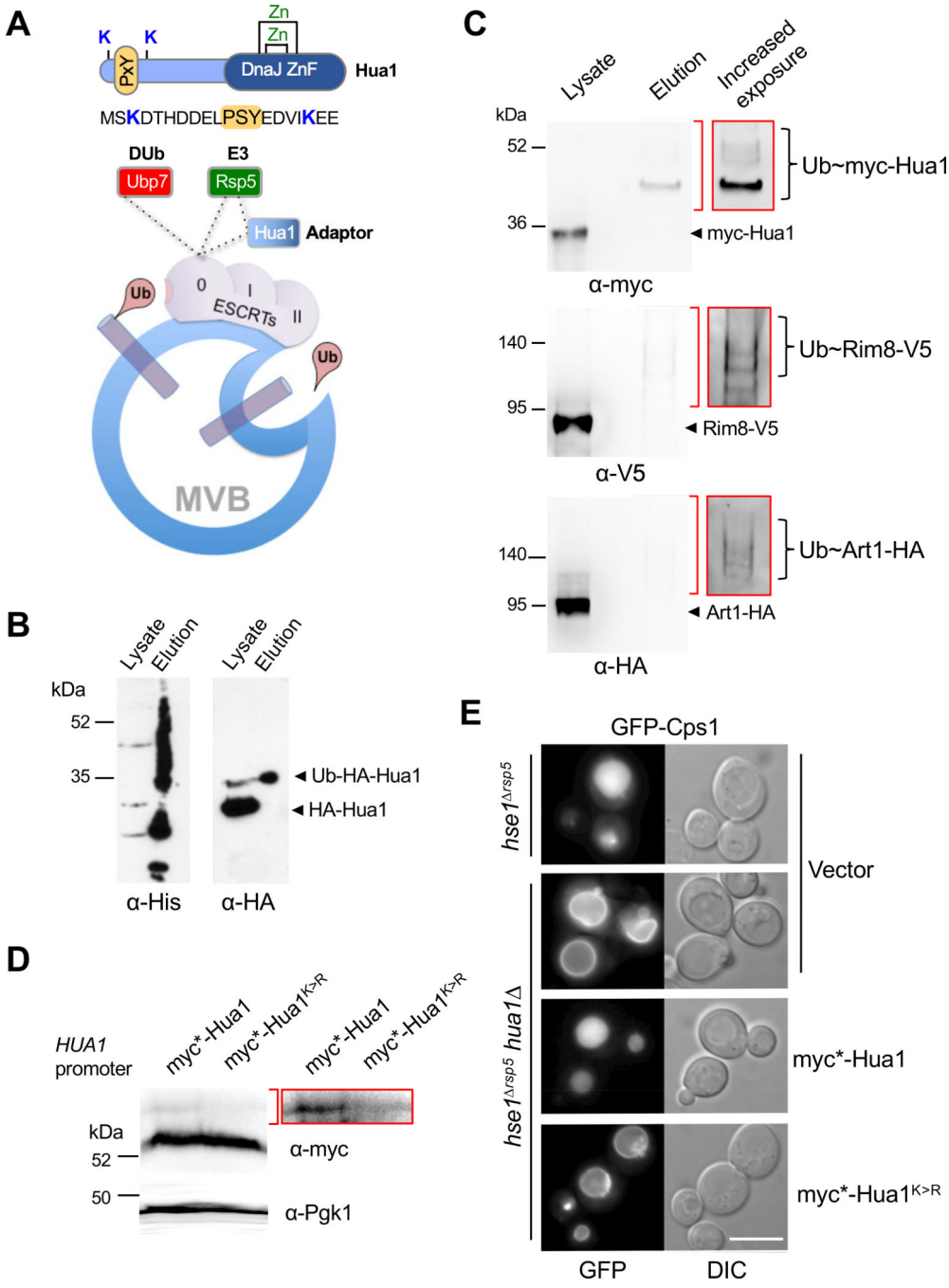

Figure 1: Ubiquitination of Hua1 is required for its role in sorting cargo to the vacuole

A) Schematic of Hua1 structure showing C-terminal zinc-finger (ZnF) domain, similar to Type I DnaJ proteins, and an N-terminal region that contains a [L/P]PxY interaction motif and ubiquitinated lysines, K_3 and K_{18} (top) and function (bottom). The ESCRT apparatus sorts ubiquitinated membrane proteins into endosomal intralumenal vesicles. The E3 ligase Rsp5 associates with the Ub-receptor complex ESCRT-0 component Hse1, both directly and indirectly via association with Hua1. A schematic of Hse1 is shown in Figure S1A.

B) HA-epitope tagged Hua1 was expressed in cells from the *CUP1* promoter with the addition of 20 μM $CuCl_2$ in cells expressing 6xHis-Ub. Ubiquitinated proteins were purified from a denatured lysate containing 8M urea over Ni-NTA agarose, eluted and immunoblotted for Ub (α-His) and Hua1 (α-HA). Both the HA-Hua1 and a slower migrating species of Hua1 corresponding to a mono-ubiquitinated form are observed in whole lysates, whereas only the latter was recovered from the Ni-NTA affinity column.
C) The same procedure described in (B) was used to analyze ubiquitination of myc-epitope-tagged Hua1, V5-epitope-tagged Rim8, and HA-epitope-tagged Art1, all expressed from low-copy plasmids from the *CUP1* promoter using 20μM $CuCl_2$. Increased exposure of the relevant region of interest from the same acquisition is outlined in red.
D) Levels of myc*-Hua1 and myc*-Hua1$^{K>R}$ (K_3R, $K_{18}R$) expressed at endogenous levels from the *HUA1* promoter was by assessed by immunoblotting whole cell lysates. Insert shows overexposure of ubiquitinated species. The myc* epitope lacking lysine was EQRLISEEDL. Increased exposure of the relevant region of interest is outlined in red. These data are extended in Figure S1B,C.
E) Fluorescence microscopy of GFP-Cps1 in cells expressing the *hse1^{Δrsp5}* mutant alone or in combination with *hua1Δ* deletion (*hua1Δ hse1^{Δrsp5}*) and co-expressing indicated forms of Hua1 from low-copy plasmids under the endogenous *HUA1* promoter.
Scale bar, 5μM. See also Table S1 for strains, antibodies, and plasmids used.

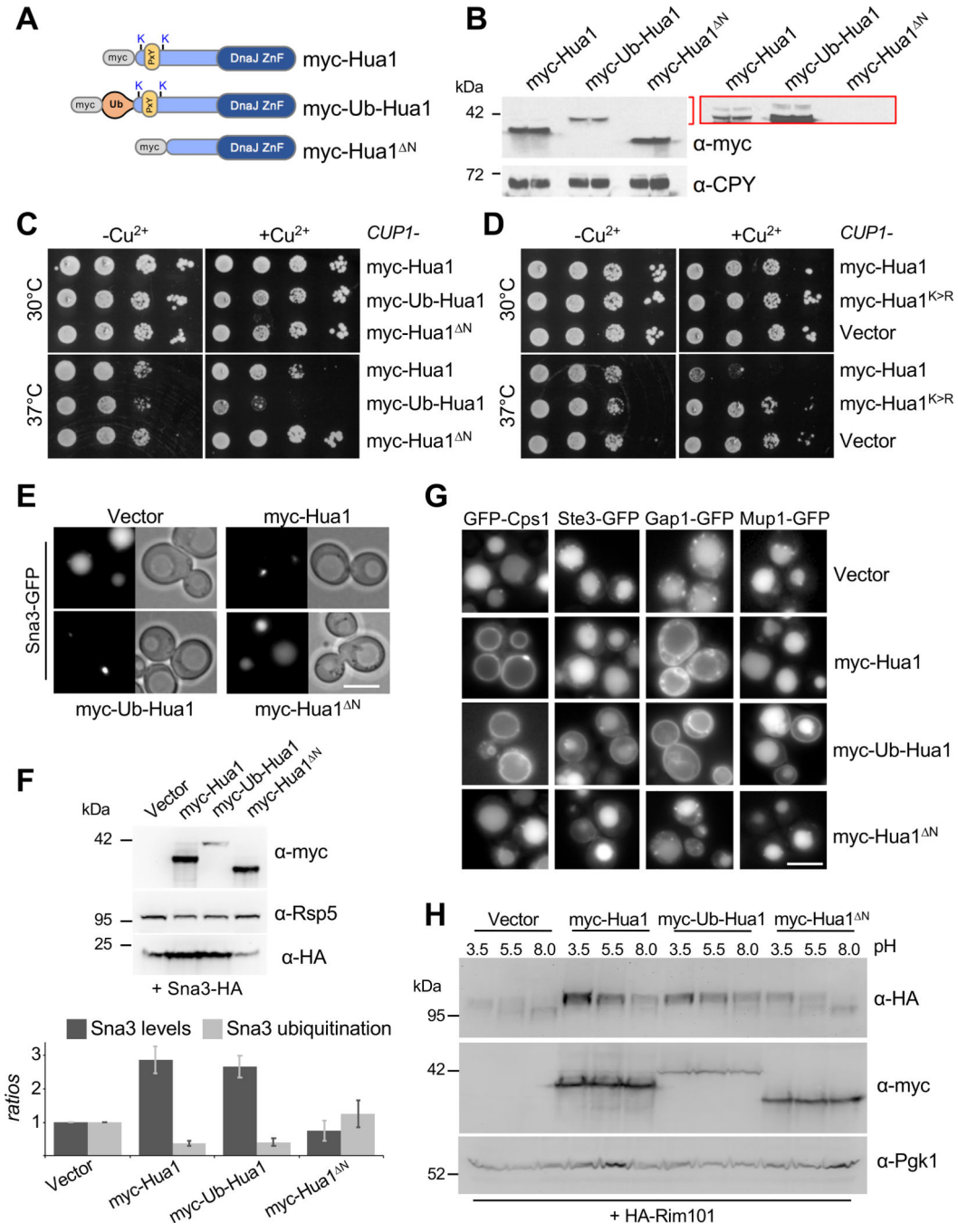

Figure 2. Overexpressing Hua1 diminishes Rsp5-dependent functions

A) Schematic of Hua1 proteins for overexpression including myc-tagged wild-type full-length protein (myc-Hua1), Ubiquitin (Ub)1–75 fused to the N-terminus of full-length Hua1 (myc-Ub-Hua1), and a truncation mutant lacking the first 20 residues (Hua1$^{\Delta N}$).

B) Levels of myc-tagged Hua1 proteins in (A) expressed from low copy plasmids under the control of the copper-inducible *CUP1* promoter assessed by immunoblotting equal amounts of whole cell lysate, shown with α-CPY control, in cells grown in the presence of 50 μM $CuCl_2$. Increased exposure (red) allows Ub bands to be visualized. Increased exposure of the

relevant region of interest is outlined in red. (Additional uncropped exposures shown in Figure S1D).

C) Growth of wild-type cells carrying the indicated Hua1 expression plasmids in the presence and absence of 50 μM $CuCl_2$ at either 30°C or 37°C. Additional conditions grow n in different CuCl2 concentrations are shown in Figure S1E.

D) Growth of wild-type cells carrying the Hua1, Hua1$^{K>R}$ expression plasmids, or vector control, in the presence and absence of 50 μM $CuCl_2$ at either 30°C or 37°C.

E) Vacuolar sorting of Sna3-GFP was assessed in wild-type (WT) cells expressing indicated Hua1 plasmids.

F) Cells expressing indicated myc tagged Hua1 plasmids were co-expressed with Sna3-HA and grown to late log phase to induce efficient vacuolar sorting before lysate generation and immuoblotting with indicated antibodies. Figure S2A shows same experiment with addition of CPY immunoblotting and Figure S2B shows results from different levels of CuCl2 induction. Below, quantitation of the relative levels of Sna3 and the proportion ubiqitinated was from separate experiments (examples shown in Figure S2C). The level of unmodified Sna3 was normalized CPY loading controls and compared to vector control cells; the proportion of ubiquitinated Sna3 was calculated by the ratio of Sna3 ubiquitinated bands vs total Sna3 and normalized to vector control (mean +/− SD, n=4).

G) Sorting of GFP-Cps1, Gap1-GFP, Ste3-GFP, and Mup1-GFP in wild-type cells (Vector) or wild-type cells expressing myc-tagged Hua1 plasmids and grown media containing 50 μM $CuCl_2$. Cells expressing Mup1-GFP were grown in the presence of 20 μg/ml methionine for 1 hr prior to imaging.

H) Cells expressing HA-Rim101 were grown to mid-log phase before shifting to buffer of indicated pH for 25 min at 30°C prior to immediate generation of lysates. HA-Rim101 processing was assessed by immunoblot from cells overexpressing Hua1 plasmids in the presence of 50 μM $CuCl_2$, or co-transformed with a vector control plasmid. The effects of Hua1 overexpression in different strains and conditions is shown in Figure S3A,B.

Scale bar, 5μM. See also Table S1 for strains, antibodies, and plasmids used.

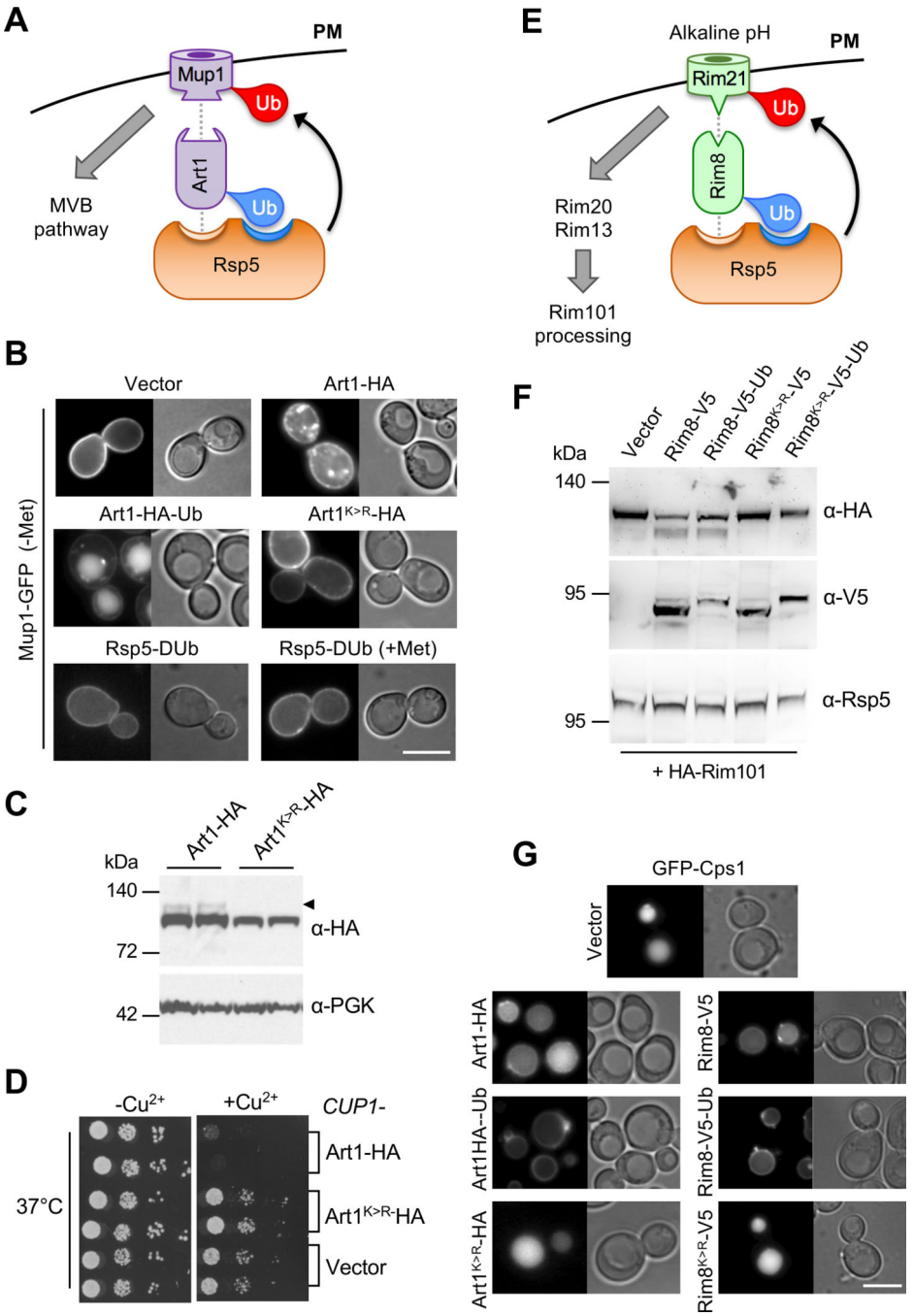

Figure 3. Different adaptors compete for residency on Rsp5

A) Schematic showing the ubiquitination of Mup1 via the cognate adaptor Art1, which is activated by its own ubiquitination.

B) Mup1-GFP expressed in wild-type cells grown to mid-log phase was localized following over-expression of indicated plasmids from the *CUP1* promoter in the presence of 50 μM $CuCl_2$.

C) The levels of Art1-HA and Art1$^{K>R}$-HA were assessed by immunoblot, with ubiquitinated species indicated (arrowhead). Figure S2D shows complementary data for monoubiquitiation of Art1-HA.

D) Growth of WT cells expressing wild-type Art1 or Art1$^{K>R}$($K_{466}R$) from the *CUP1* promoter within low-copy plasmids or transformed with vector control.

E) Schematic showing processing of Rim101 is mediated by the ubiquitination of Rim21 by its cognate adaptor Rim8, activity of which itself is regulated by ubiquitination and ligase residency.

F) HA-Rim101 levels were assessed in buffered media in the presence of indicated variants of Rim8 over-expressed from the *CUP1* promoter.

G) Localization of GFP-Cps1 in wild-type cells at mid-log phase with over-expressed adaptors.

Scale bar, 5μM. See also Table S1 for strains, antibodies, and plasmids used.

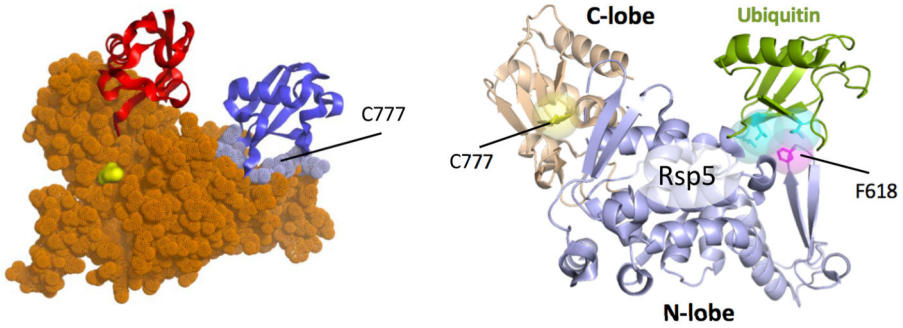

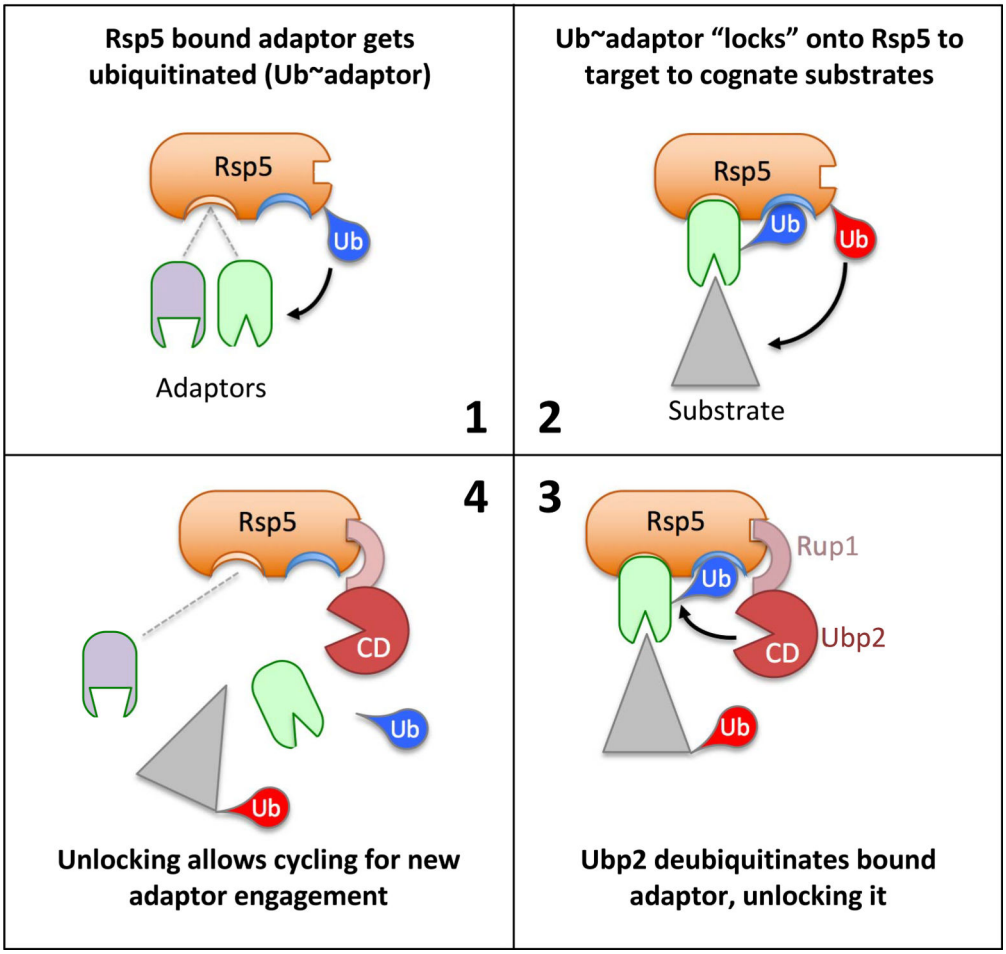

Figure 4. Cycle of ubiquitination to control adaptor function

Above are structural models (based on PDB: 4LCD and 3OLM) for the Rsp5 HECT domain interacting covalently and non-covalently with Ub. Highlighted is the position of F618, critical for Ub-binding. Below is a proposed model whereby different adaptors compete to occupy Rsp5. Initial binding of an adaptor results in its ubiquitination (1), which allows the ubiquitinated adaptor to bind tighter by also engaging the N-lobe Ubiquitin Binding Surface (UBS). This tight adaptor/Rsp5 complex is now more dedicated towards the specific substrates targeted by the adaptor (2). To 'unlock' ubiquitinated adaptors from Rsp5, Ubp2

is recruited to the complex via Rup1 and deubiquitinates adaptors (3), allowing them to disengage from Rsp5 and allow other adaptors to bind Rsp5 (4).

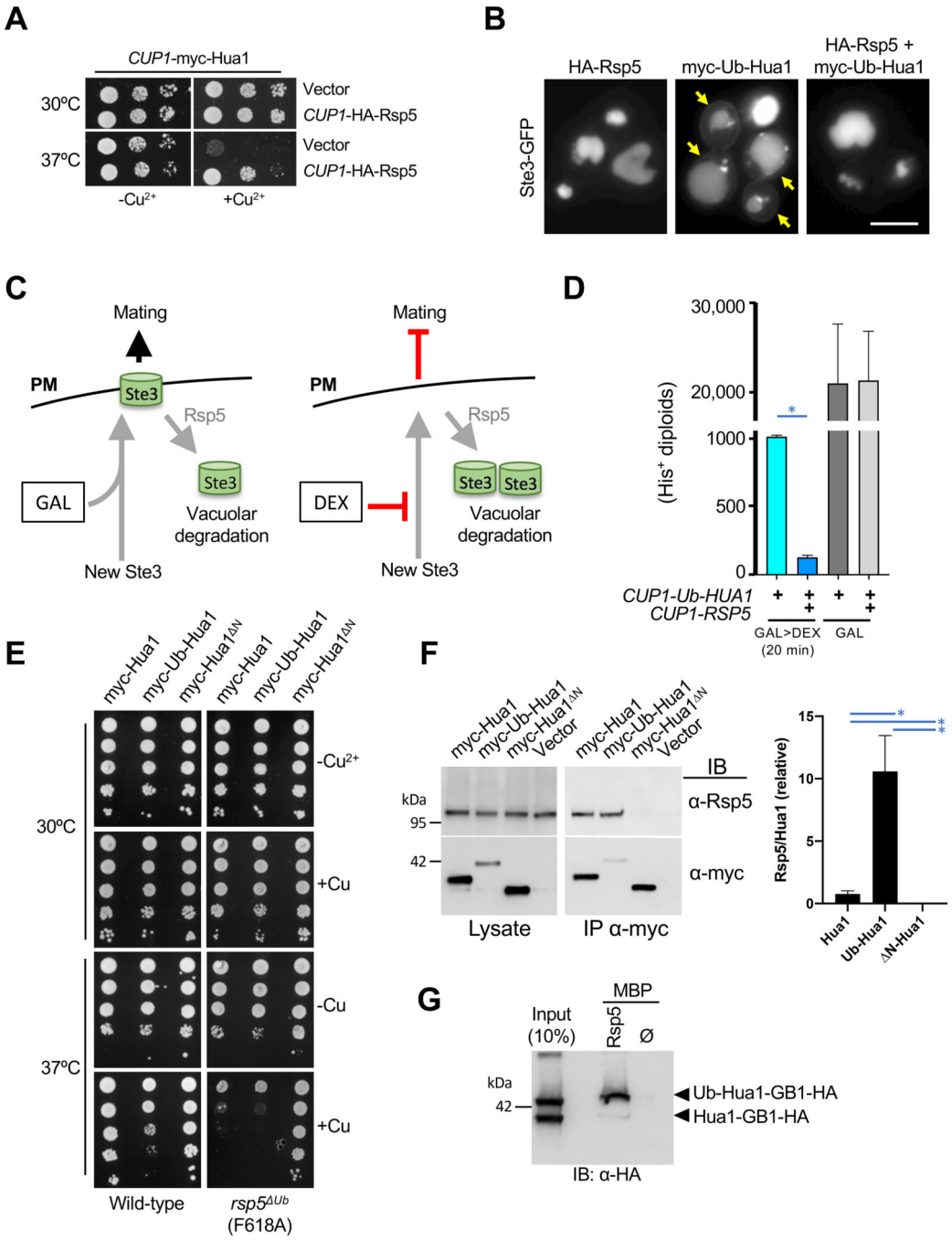

Figure 5. Rsp5 levels suppress defects due to competing adaptors

A) Growth of WT cells at 30°C and 37°C overexpressing Hua1 in the presence and absence of Rsp5 overexpression. Hua1 and HA-tagged Rsp5 were expressed from the *CUP1* promoter with low copy plasmids in the presence and absence of 50 μM added $CuCl_2$.

B) Sorting of Ste3-GFP in WT cells grown in 30 μM $CuCl_2$ expressing myc-Ub-Hua1 and/or HA-Rsp5 from the *CUP1* promoter within low-copy plasmids.

C) Schematic rationale for the mating assay in (D). Once newly synthesized Ste3 is terminated by shifting cells to glucose, mating can only be sustained by residual cell-surface Ste3 which is constitutively downregulated by Rsp5.

D) MAT**α** *his3* cells expressing Ste3-HA from the dextrose-repressible *GAL1* promoter and expressing Ub-Hua1 under control of *CUP1* promoter in presence of 50 μM copper were grown overnight in galactose media (GAL). Dextrose (DEX) was added or not for 20 min prior to mating with MAT>**a** *his4* cells in rich media containing GAL or DEX. Cells were then pelleted, diluted, and spread on -His plates to select for diploid cells. The number of diploids from each plate were counted after 2 days growth and plotted. The *GAL-STE3-HA* MAT**α** cells were also expressing either HA-Rsp5 or vector alone (*=$p<0.05$). Additional data using this assay are shown in Figure S3E.

E) Growth of WT cells or cells carrying the $rsp5^{\Delta Ub}$ allele ($F_{618}A$ mutation blocking the N-lobe UBD) that were expressing myc-tagged Hua1, Ub-Hua1, or $Hua1^{\Delta N}$ from the *CUP1* promoter within low-copy plasmids. Growth was monitored at 30°C and 37° C in the presence and absence of added $CuCl_2$ (50μM).

F) Lysates from cells transformed with vector alone or that overexpressed myc-tagged Hua1, Ub-Hua1, and $Hua1^{\Delta N}$ were immunoprecipitated with anti-myc polyclonal antibodies. Lysates (left) and immunoprecipitates (middle) were immunoblotted with polyclonal antibodies to Rsp5 or myc. Right shows quantitation of the ratio of Rsp5 to the level of immunoprecipitated Hua1 variant used calculated from 3 separate groups of transformants shown in Figure S3C (mean, +/−SD, n=3) anti-GST-polyclonal antibodies and immunoblotted with anti-HA and anti-myc antibodies. HA-Rsp5 was expressed from *RSP5* promoter, Hua1 variants were expressed from the *CUP1* promoter. Below shows the relative ratio of HA:myc immunoreactivity within the myc-Hua1 immunoprecipitations. Scale bar, 5μM. Immunoprecipitation data using Rsp5 lacking its N-lobe Ub-binding surface is shown in Figure S3D.

G) Hua1 and Ub-Hua1 were produced in bacteria as fusion proteins with GB1 that carried an C-terminal HA tag. Lysates were mixed and incubated with beads coated with MBP alone (Ø) or a MBP-Rsp5 fusion protein. Beads were washed and immunoblotted with anti-HA along with a 10% equivalent of the pooled input lysate.

See also Table S1 for strains, antibodies, and plasmids used.

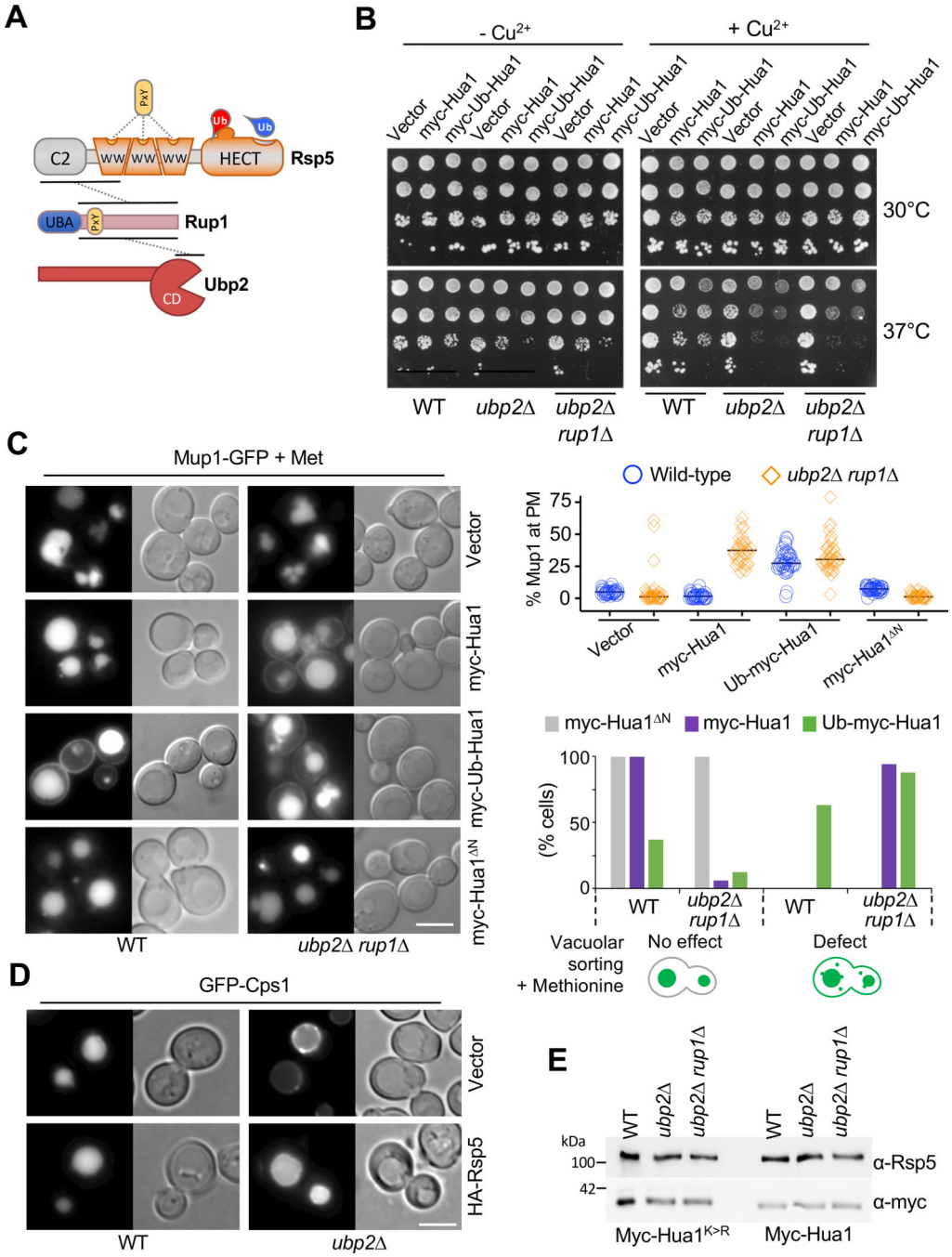

Figure 6. Loss of Ubp2 increases potency of Hua1 as a competitive inhibitor

A) Schematic of the complex Rsp5 forms with Rup1 and Ubp2. The 3 WW domains of Rsp5 interact with PY motifs present in substrates and adaptors. Rup1, which has a PY motif, recruits the deubiquitinating enzyme Ubp2 to Rsp5. Areas sufficient for protein:protein interactions are indicated by horizontal line. Also cartooned are two bound Ub molecules within the catalytic HECT domain, one that is carried by the active site cysteine for transfer to substrates (red) and another bound non-covalently to the N-lobe UBD (blue).

B) Growth of WT, *ubp2*Δ and *ubp2Δ rup1Δ* cells expressing myc-tagged Hua1 and Ub-Hua1 from the *CUP1* promoter within low-copy plasmids at 30°C and 37°C in the presence and absence of 50 μM $CuCl_2$.

C) Sorting of Mup1-GFP in WT or *ubp2Δ rup1Δ* cells overexpressing myc-tagged Hua1, Ub-Hua1, and $Hua1^{\Delta N}$. Cells were grown in SD media containing 50 μM $CuCl_2$ and 20 μg/ml methionine for 1hr. Representative micrographs are shown (left) with quantitation across multiple cells/experiments (right). Top quantitation shows percent of Mup1 at the cell surface individually for multiple cells along with the average value (line). Below quantitation shows the proportion of cells that showed the indicated schematic phenotype wherein methionine-induced downregulation was unperturbed and all cells showed Mup1 exclusively in the vacuole, vs defective downregulation where Mup1 was also observed in non-vacuolar compartments (cell surface and endosomes). Number (N) of WT cells counted expressing Hua1, Ub-Hua1, and $Hua1^{\Delta N}$ was 41,133,112. N for *ubp2Δ rup1Δ* cells was 177, 209, and 113, respectively.. Statistical significance for these levels are provided in Figure S4A.

D) Sorting of GFP-Cps1 in wild-type and *ubp2*Δ cells in the presence and absence of overexpression of HA-Rsp5 from the *CUP1* promoter in cells grown in 10 μM $CuCl_2$.

E) Immunoblot of WT, *ubp2*Δ, and *ubp2Δ rup1Δ* cells expressing myc*-Hua1 and myc*-$Hua1^{K>R}$ from endogenous *HUA1* promoter, with an Rsp5 immunoblot as loading control. An expanded dataset with quantitation is shown in Figure S4B.

Scale bar, 5μM. See also Table S1 for strains, antibodies, and plasmids used.

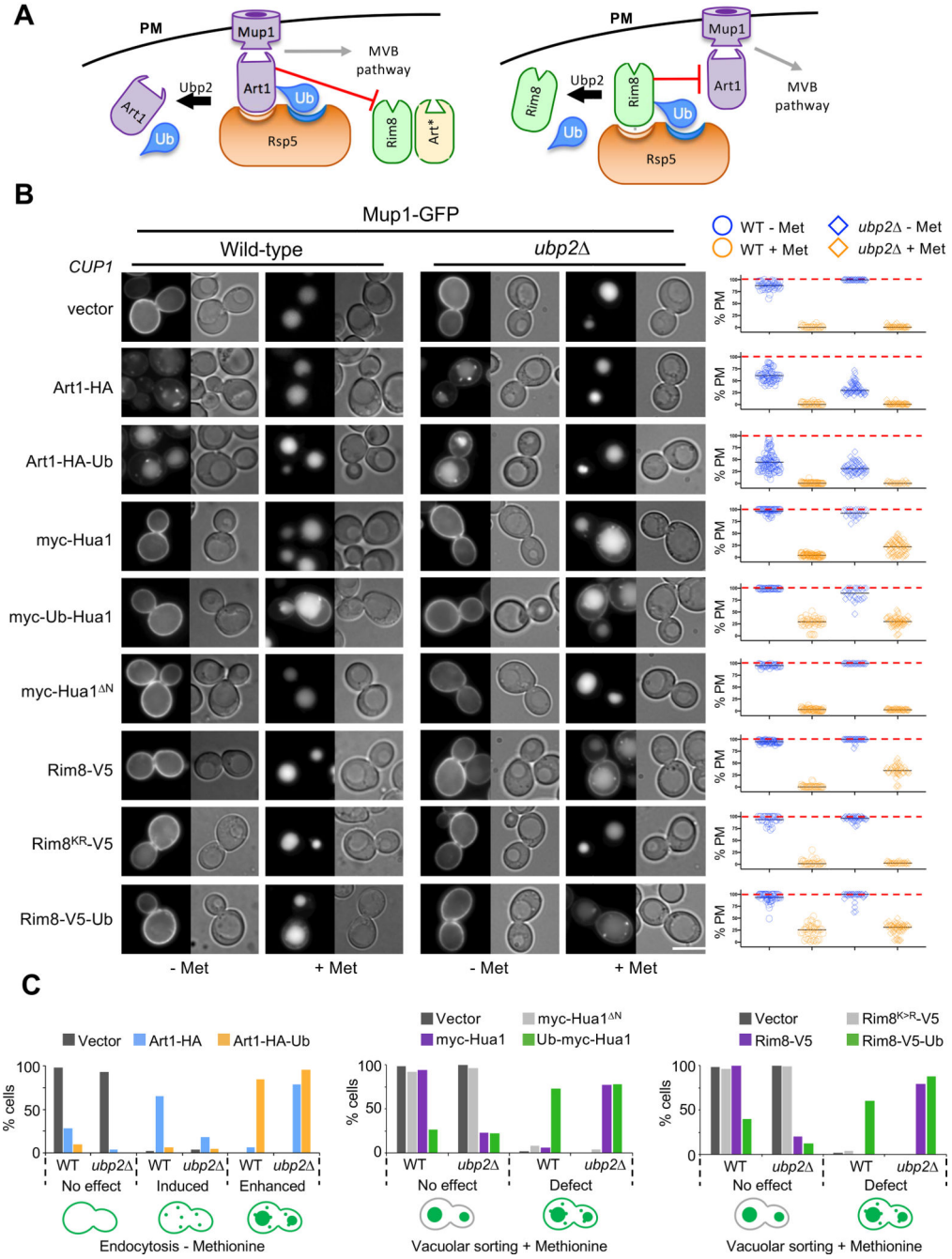

Figure 7. Effects of competition and Ubp2 on adaptor cycling

A) Schematic depicting the activity of ubiquitinated Art1 towards promoting downregulation of its cognate substrate Mup1 while also diminishing the activity other adaptors towards other cargoes that are not regulated by Art1 (left). Schematic depicting how ubiquitinated Rim8 will occupy Rsp5 and inhibit the ability of Art1 to mediate ubiquitination and trafficking of Mup1 into the MVB pathway (right). In each case, adaptor cycling can be achieved through the enzymatic activity of Ubp2.

B) Cells were imaged prior to (− Met) or following (+ Met) 1 h treatment with methionine. Mup1-GFP was localized in WT (left) and *ubp2Δ* (right) cells grown to mid-log phase in the presence of indicated *CUP1* over-expression plasmids. Quantitation of percent of Mup1 at the cell surface individually for multiple cells along with the average value (line) indicated (far right). Statistical significance for each comparison is summarized in Figure S4C. Scale bar, 5μM.

C) Quantification of morphological profile for Mup1-GFP localization from data in (D) in the absence and presence of methionine. Left shows number of cells with exclusively cell surface distribution, distribution in endosomes, or distribution within the vacuole of cells grown in the absence of methionine and overexpressing the indicated forms of Art1. N=131,175,121,182 For Vector, Art1-HA, Art1-HA-Ub: N (WT) = 131,121,182, 175; N (*ubp2Δ*) = 96,138,100.

Middle shows number of cells with exclusively vacuolar localization (normal/ no effect) or defective localization with some in endosomes and cell surface after a 1hr treatment with methionine for cells overexpressing indicated Hua1 variants. Right shows cells with normal and defective distribution of Mup1 in cells overexpressing indicated variants of Rim8. For Vector, Rim8-V5, Rim8-V5$^{K>R}$, Rim8-V5-Ub, myc-Hua1, myc-Hua1$^{\Delta N}$, myc-Ub-Hua1: N(WT) = 152,62,80,121,241,288,172 and N(*ubp2Δ)* = 118,117,131,104,117,103,161. See also Table S1 for strains, antibodies, and plasmids used.

Key resource table:

REAGENT or RESOURCE	SOURCE	IDENTIFIER
Antibodies		
α-HA. Mouse Monoclonal (HA.11).	Biolegend, SanDiego, CA	Cat# HA.11
α-myc. Rabbit Polyclonal.	QED Biosciences Inc., San Diego, CA	Cat# 18826
α-myc. Mouse Monoclonal (THE™-myc Tag).	Genscript, Piscataway, NJ	Cat# A00704
α-6xHis. Mouse Monoclonal (THE™-His Tag).	Genscript, Piscataway, NJ	Cat# A00174-40
α-PGK. Mouse Monoclonal	Molecular Probes	Cat# 459250
α-V5. Mouse Monoclonal.	Invitrogen, ThermoFisher	Cat# R960-25
α-CPY. Mouse Monoclonal antibody (10A5-B5)	Invitrogen, ThermoFisher	Cat# A-6428
α-Rsp5. Rabbit Polyclonal antibody	[51]	N/A
α-GST. Rabbit Polyclonal antibody	[52]	N/A
α-myc. Goat Polyclonal antibody conjugated to sepharose	QED Biosciences Inc., San Diego, CA	Cat# 18824A
Bacterial and Virus Strains		
BL21 (DE3) E. coli. fhuA2 [lon] ompT gal (λ DE3) [dcm] ΔhsdS λ DE3 = λ sBamHIo ΔEcoRI-B int::(lacI::PlacUV5::T7 qene1) i21 Δnin5	New England Biolabs, MA	Cat# C2527H
MC1061 E. coli. araD139 Del(araA-leu)7697 Del(lac)X74 galK16 galE15(GalS) lambda- e14- mcrA0 relA1 rpsL150(strR) spoT1 mcrB1 hsdR2	[53]	N/A
Biological Samples		
No critical biological samples		
Chemicals, Peptides, and Recombinant Proteins		
Peptone	RPI, Mt Prospect, IL	Cat# P200248
Yeast Extract	RPI, Mt Prospect, IL	Cat# Y20020
Tryptone	RPI, Mt Prospect, IL	Cat# T60060
Yeast Nitrogen Base	RPI, Mt Prospect, IL	Cat# Y20040
Dextose	RPI, Mt Prospect, IL	Cat# G32045
NaCl	RPI, Mt Prospect, IL	Cat# S23025
Urea	RPI, Mt Prospect, IL	Cat#U20200

REAGENT or RESOURCE	SOURCE	IDENTIFIER
Bacto Agar	Becton Dickenson, Sparks MD	Cat# 214010
Amino Acid supplements	Formedium, Hunstanton, UK	Custom
Galactose	Sigma, St. Louis, MO	Cat# G0625
Complete Protease Inhibitor	Sigma, St. Louis, MO	Cat# 11697498001
Critical Commercial Assays		
No critical commercial assays		
Deposited Data		
No other datasets		
Experimental Models: Cell Lines		
None		
Experimental Models: Organisms/Strains		
(PLY1877) BY4742 Wild-type; MAT**α**, *his3Δ1 leu2Δ0 lys2Δ0 ura3Δ0*	[54]	N/A
(PLY355) SEY6210 Wild-type; MAT**α**, *leu2-3,112 ura3-52 his3-Δ200 trp1-Δ901 lys2-801 suc2-Δ9*	[55]	N/A
(PLY4272) BY4742; *pdr5Δ::loxP hbt1$^{\Delta C}$::loxP ubi4Δ::TEF1*-6xHis-ALINQERA-Ub-his5+*	[56]	N/A
(PLY3173) BY4742; *hse1$^{\Delta rsp5}$::HIS3 (P(445)PPGYEQ>**AAA**GYEQ)*	[21]	N/A
(PLY3469) BY4742; *hua1Δ::kan^r hse1$^{\Delta rsp5}$::HIS3*	This manuscript	N/A
(PLY2463) SEY6210; *pep4Δ*	[57]	N/A
(PLY4804) *STE3-5'UTRΔ::kan^r-GAL1*-3xHA-Ste3	This manuscript	N/A
(PLY42) SF838-9Da Wild-type MAT**a** *leu2-3,112, ura3-52, his4-519, ade6*	[58]	N/A
(PLY4072) *his3 leu2 ura3 trp1 bar1 rsp5Δ::HIS3* with pRsp5-*TRP1* plasmid (LHW1103)	[59]	N/A
(PLY4074) *his3 leu2 ura3 trp1 bar1 rsp5Δ::HIS3* with pRsp5-F618A-*TRP1* plasmid (LHY2737)	[23]	N/A
(PLY3923) *ubp2Δ::kan^r*	This manuscript	N/A
(PLY3927) *ubp2Δ::kan^r rup1Δ::his5+*	This manuscript	N/A
(PLY5709) *rup1Δ::kan^r*	This manuscript	N/A
(PLY4151) *hua1Δ::kan^r*	[21]	N/A
Oligonucleotides		
There are no oligonucleotides critical for the reproduction of these experiments		
Recombinant DNA		
HA epitope tag = YPYDVPDYA	[60]	N/A
myc epitope tag = EQKLISEEDL	[61]	N/A
myc* epitope tag = EQRLISEEDL	[62]	N/A
V5 epitope tag = GKPIPNPLLGLDST	[63]	N/A

REAGENT or RESOURCE	SOURCE	IDENTIFIER
His tag = HHHHHH	[64]	N/A
Ub = ubiquitin residues 1- 75 = codons for: MQIFVKTLTGKTITLEVEPSDTIENVKAKIQDKEGIPPDQQRLIFAGKQLEDGRTLSDYNIQKESTLHLVLRLRG	Uniprot	UBC_Human
(pPL82) *URA3* containing low copy *CEN* plasmid (pRS316)	[65]	N/A
(pPL83) *LEU2* containing low copy *CEN* plasmid (pRS315)	[65]	N/A
(pPL138) *HIS3* containing low copy *CEN* plasmid (pRS313)	[65]	N/A
(pPL4418) pRS316 expressing 3xHA-Hua1 from *TEF1* promoter	This manuscript	N/A
(pPL4390) pRS316 expressing myc-Hua1 from *CUP1* promoter	This manuscript	N/A
(pPL6419) pRS316 expressing Rim8-3xV5 from *CUP1* promoter	This manuscript	N/A
(pPL5468) pRS316 expressing myc*-Hua1 from *HUA1* promoter	This manuscript	N/A
(pPL5467) pRS316 expressing myc*-Hua1$^{K>R}$(K3R K18R) from *HUA1* promoter	This manuscript	N/A
(pPL1857) pRS16 expressing GFP-Cps1 from *PRC1* promoter (pGO45)	[66]	N/A
(pPL4392) pRS316 expressing Ub-myc-Hua1 from *CUP1* promoter	This manuscript	N/A
(pPL4394) pRS316 expressing myc-Hua1$^{\Delta N}$ (Hua1 21-198) from *CUP1* promoter	This manuscript	N/A
(pPL2089) pRS315 expressing Sna3-GFP from *SNA3* promoter	[35]	N/A
(pPL6151) pRS315 expressing Sna3-2xHA from *SNA3* promoter	This manuscript	N/A
(pPL2572) pRS315 expressing GFP-Cps1 from *PRC1* promoter	This manuscript	N/A
(pPL967) pRS315 expressing Ste3-GFP from *STE3* promoter	[67]	N/A
(pPL2334) pRS315 expressing Gap1-GFP from *CUP1* promoter	[44]	N/A
(pPL4069) pRS315 expressing Mup1-GFP from *MUP1* promoter	[44]	N/A
(pPL3109). pRS315 expressing 3xHA-Rim101 from *????* promoter (pFL1)	[68]	N/A
(pPL6419) pRS316 expressing Rim8-3xV5 from *CUP1* promoter	This manuscript	N/A
(pPL6462) pRS316 expressing Rim8-3xV5-Ub from *CUP1* promoter	This manuscript	N/A
(pPL6414) pRS316 expressing Rim8-3xV5$^{K>R}$(K521R) from *CUP1* promoter	This manuscript	N/A
(pPL6413) pRS316 expressing Rim8-3xV5$^{K>R}$(K521R)-Ub from *CUP1* promoter	This manuscript	N/A
(pPL5081) pRS315 expressing 3xHA-Rsp5 from *CUP1* promoter	This manuscript	N/A
(pPL991) pRS313 expressing Ste3-GFP from *STE3* promoter	[44]	N/A
(p5642) YCplac33 expressing HA-Rsp5 from *RSP5* promoter	[69]	N/A
(p5797) pET28MBP expressing 6xHis-MBP-Rsp5 from *T7* promoter (pJL242)	[27]	N/A
(pPL6374) pET21a expressing Hua1-GB1-HA-6xHis from *T7* promoter	This manuscript	N/A
(pPL6373) pET21a expressing Ub-Hua1-GB1-HA-6xHis from *T7* promoter	This manuscript	N/A

REAGENT or RESOURCE	SOURCE	IDENTIFIER
(pPL4626) pRS316 expressing myc*-Hua1 from *CUP1* promoter	This manuscript	N/A
(pPL4628) pRS316 expressing myc*-Hua1$^{K>R}$ from *CUP1* promoter	This manuscript	N/A
pMAL. Maltose-binding protein expression plasmid	New England Biolabs, MA	Cat# E8200S
Software and Algorithms		
Adobe Photoshop.	Adobe	https://www.adobe.com/creativecloud/business/enterprise.html?promoid=NV3KR73Y&mv=other
Microsoft Office.	Microsoft	https://www.office.com
Lasergene.	DNAstar	https://www.dnastar.com/software/
Pymol.	Schrödinger	https://pymol.org/2/
Fiji	Eliceiri/LOCI group University of Wisconsin-Madison	https://fiji.sc
Prism8.	GraphPad	https://www.graphpad.com/scientific-software/prism/
Other		
One-Shot, cell disruptor	Constant Systems Ltd Daventry Northants, UK	http://www.constantsystems.com/products/oneshot.php